AMERICAN SOCIETY FOR MICROBIOLOGY | Journal of Bacteriology

Editor's Pick | Bacteriology | Full-Length Text

A riboswitch-controlled TerC family transporter Alx tunes intracellular manganese concentration in *Escherichia coli* at alkaline pH

Ravish Sharma,[1] **Tatiana V. Mishanina**[1]

AUTHOR AFFILIATION See affiliation list on p. 19.

ABSTRACT Cells use transition metal ions as structural components of biomolecules and cofactors in enzymatic reactions, making transition metal ions integral cellular components. Organisms optimize metal ion concentration to meet cellular needs by regulating the expression of proteins that import and export that metal ion, often in a metal ion concentration-dependent manner. One such regulation mechanism is via riboswitches, which are 5′-untranslated regions of an mRNA that undergo conformational changes to promote or inhibit the expression of the downstream gene, commonly in response to a ligand. The *yybP-ykoY* family of bacterial riboswitches shares a conserved aptamer domain that binds manganese ions (Mn^{2+}). In *Escherichia coli*, the *yybP-ykoY* riboswitch precedes and regulates the expression of two different genes: *mntP*, which based on genetic evidence encodes an Mn^{2+} exporter, and *alx*, which encodes a putative metal ion transporter whose cognate ligand is currently in question. The expression of *alx* is upregulated by both elevated concentrations of Mn^{2+} and alkaline pH. With metal ion measurements and gene expression studies, we demonstrate that the alkalinization of media increases the cytoplasmic manganese pool, which, in turn, enhances *alx* expression. The Alx-mediated Mn^{2+} export prevents the toxic buildup of the cellular manganese, with the export activity maximal at alkaline pH. We pinpoint a set of acidic residues in the predicted transmembrane segments of Alx that play a critical role in Mn^{2+} export. We propose that Alx-mediated Mn^{2+} export serves as a primary protective mechanism that fine tunes the cytoplasmic manganese content, especially during alkaline stress.

IMPORTANCE Bacteria use clever ways to tune gene expression upon encountering certain environmental stresses, such as alkaline pH in parts of the human gut and high concentration of a transition metal ion manganese. One way by which bacteria regulate the expression of their genes is through the 5′-untranslated regions of messenger RNA called riboswitches that bind ligands to turn expression of genes on/off. In this work, we have investigated the roles and regulation of *alx* and *mntP*, the two genes in *Escherichia coli* regulated by the *yybP-ykoY* riboswitches, in alkaline pH and high concentration of Mn^{2+}. This work highlights the intricate ways through which bacteria adapt to their surroundings, utilizing riboregulatory mechanisms to maintain Mn^{2+} levels amidst varying environmental factors.

KEYWORDS *yybP-ykoY*, riboswitches, exporters, TerC family, manganese, *alx*, *mntP*

Transition metals are essential in all organisms as structural elements of proteins and RNA and as reactive centers in enzymes. Among these metals, iron (Fe^{2+}) acts as a cofactor in many cellular enzymes essential for life, e.g., those involved in respiratory pathways. During aerobic growth or in response to oxidizing agents such as hydrogen

Editor Conrad W. Mullineaux, Queen Mary University of London, London, United Kingdom

Address correspondence to Tatiana V. Mishanina, tmishanina@ucsd.edu.

The authors declare no conflict of interest.

See the funding table on p. 20.

Received 19 April 2024
Accepted 11 May 2024
Published 13 June 2024

peroxide (H_2O_2), cells generate reactive oxygen species (ROS) that can oxidize Fe^{2+}, thereby inactivating Fe^{2+}-dependent enzymes and leading to cytotoxic effects if not treated. To counter ROS-caused negative consequences, *Escherichia coli* (*E. coli*) relies on an Mn^{2+}-dependent isoenzyme of superoxide dismutase (SOD), an enzyme that converts highly reactive superoxide radicals to molecular oxygen and H_2O_2: cytosolic Mn^{2+}-dependent SodA takes over in aerobic conditions when the activity of Fe^{2+}-dependent SodB is insufficient to scavenge superoxide (1).

To be ready for an impending ROS threat, *E. coli* maintain a constant cellular pool of manganese through the uptake activity of the only characterized Mn^{2+} importer, MntH (2, 3). The total cellular concentration of manganese (Mn, free and bound) is estimated to be 15–21 µM by inductively coupled plasma mass spectrometry (ICP-MS) measurements (4–6). MntH uses conserved acidic transmembrane residues to coordinate Mn^{2+} for import and relies on a proton gradient across the inner membrane of an *E. coli* cell as a driving force for Mn^{2+} uptake (7–10). A low-affinity Zn^{2+} transporter, ZupT, in *E. coli* was also reported to uptake Mn^{2+} along with Fe^{2+}, Cd^{2+}, and Co^{2+} (11, 12). Notwithstanding its critical role within the cell, Mn^{2+} concentration ([Mn^{2+}]) must be limited as it is toxic to the cell in high concentrations. Excess Mn^{2+} replaces similarly sized Fe^{2+} as a cofactor in enzymes and can alter levels of other metal ions (4, 5). To prevent the toxic buildup of Mn^{2+}, the expression of *mntH* is repressed by elevated [Mn^{2+}] and an Mn^{2+}-dependent transcriptional regulator MntR (3, 13). As an additional protective measure, excess Mn^{2+} is transported out of *E. coli* by its only exporter characterized to date, MntP (4, 5, 13, 14). Similar to MntH, several conserved acidic residues within the membrane are implicated in the Mn^{2+} efflux activity of MntP (14). YiiP, an Fe^{2+} and Zn^{2+} exporter, is implicated in protection against Mn^{2+} intoxication in *Salmonella enterica* Serovar Typhimurium (15) and is also present in *E. coli* but not studied for its Mn^{2+} export potential.

One of the mechanisms by which *mntP* expression is tuned in response to the changing intracellular [Mn^{2+}] is via the riboswitch in the 5′ untranslated region (UTR) of the *mntP* gene. Riboswitches are *cis*-acting elements in the UTRs of mRNAs, meaning that they alter transcriptional and/or translational outcomes for that mRNA. Riboswitches do so by shifting their structural ensembles upon binding to a ligand (16). For example, ligand binding might favor folding of the riboswitch RNA into a hairpin that terminates transcription to attenuate expression of the downstream gene (transcriptional riboswitch) (17, 18). Alternatively, ligand binding can promote the mRNA with a single-stranded ribosome-binding site (RBS), thus enhancing the translation of that mRNA (translational riboswitch). The *mntP* riboswitch was characterized as a translational riboswitch where the translation is turned on in response to increased intracellular Mn (19, 20). As a member of the ubiquitous *yybP-ykoY* riboswitch family (21, 22), the *mntP* riboswitch turns on *mntP* mRNA translation by binding free Mn^{2+}. A second *yybP-ykoY* riboswitch in *E. coli* precedes a gene (*alx*) that, curiously, is highly induced in response to alkaline pH (23, 24). The expression of both *mntP* and *alx* increases in media with elevated [Mn^{2+}] (19, 20). The *alx* encodes a putative Mn^{2+} transporter that belongs to the TerC superfamily of proteins (14, 25); however, the function of the Alx protein has not been definitively established.

A prior study indicated that overexpression of Alx results in an increase in the intracellular Mn pool and suggested that Alx may act as an Mn^{2+} importer (14). This proposal, however, is contradicted by the observations from earlier reports that the expression of *alx* and *mntP* (Mn^{2+} exporter) is increased by supplemented Mn^{2+} in the media, whereas the expression of *mntH* (Mn^{2+} importer) is repressed. If Alx were, indeed, an Mn^{2+} importer, its expression in response to changing [Mn^{2+}] would have paralleled that of MntH, not MntP. Here, we present evidence that Alx is an exporter of Mn^{2+} serving as the first line of defense against the potential buildup of cytoplasmic Mn at alkaline pH. By examining the effect of alkaline intracellular pH and increased [Mn^{2+}] on *alx* expression through transcriptional and translational reporters, we show that these two environmental cues are linked. Additionally, we demonstrate that Alx activity is

stimulated by alkaline pH and posit involvement of transmembrane acidic residues of Alx in Mn^{2+} export.

RESULTS

Increased extracellular pH and Mn enhance *alx* expression

To study the connection between alkaline pH and Mn homeostasis, we employed transcriptional and translational *lacZ* reporter fusions of *alx* and *mntP* cloned with their respective native promoters into single-copy plasmids (Fig. S1A). Effects of extracellular alkaline pH and elevated extracellular [Mn^{2+}] on gene expression were measured by β-galactosidase assays in *E. coli* strain (MC4100) lacking *alx* (referred to as Δ*alx*). Briefly, the Δ*alx* strain was transformed with plasmids containing either *alx* or *mntP* transcriptional or translational reporters (Fig. S1A; Table S2). The strains were cultivated in (i) neutral pH (LBK pH 6.8) or alkaline pH (LBK pH 8.4) media to test the effect of pH on *alx* transcriptional and translational reporters as described in prior work (24) and (ii) LB (pH 6.8) with supplemented $MnCl_2$ to test the effect of Mn^{2+} on *alx* transcriptional and translational reporters. These experimental conditions were tested in parallel on *mntP* transcriptional and translational reporters (19). We observed that *alx* transcription increased 5-fold at alkaline pH (Fig. 1A), whereas *mntP* transcription increased 1.5-fold (Fig. 1A), consistent with an increase in the average rate of nucleotide addition as pH increases (26, 27). The higher increase in the *alx* vs *mntP* transcriptional reporter activity at alkaline pH can be explained by the proposed intrinsic terminator in hairpin D forming within the 5′ UTR of *alx* in neutral but not alkaline pH (19, 24) (Fig. S1B). In contrast, the *alx* translational reporter produced a striking 68-fold higher signal in alkaline pH—higher than previously observed (24), whereas the *mntP* translational reporter was unaffected by alkaline pH (Fig. 1B). These results indicate that *alx* expression is largely regulated post-transcriptionally in alkaline pH, consistent with previous work (24).

The 5′ UTR of *alx* mRNA referred to as the pH-responsive RNA element (PRE) regulates *alx* translation in response to a pH change as previously shown (24). We observed that the translational reporter of *alx* that lacks PRE (ΔPRE) exhibited only a 2-fold increase in alkaline pH vs 68-fold increase with PRE present (Fig. 1B). PRE contains two intrinsic transcription terminators (Fig. S1B), and their absence is the dominant cause of higher transcriptional output in the ΔPRE transcriptional reporter. The ΔPRE *alx* translational reporter displayed high β-galactosidase activity in both pH conditions, with a twofold increase in alkaline vs neutral pH (Fig. 1B), in good agreement with the corresponding twofold increase in ΔPRE *alx* transcription upon alkalinization (Fig. 1A). Taken together, these results show that PRE regulates both transcription and translation of *alx* in a pH-responsive manner.

Upon supplementation of $MnCl_2$ to the LB media (pH 6.8), the *alx* and *mntP* transcriptional reporter outputs increased 2.7-fold and 1.4-fold, respectively (Fig. 1C). In stark contrast, both *alx* and *mntP* translational reporters were progressively induced by increasing [Mn^{2+}], with a 21- and an 11-fold increase, respectively, at the highest $MnCl_2$ concentration tested (500 µM) (Fig. 1D). The ΔPRE translational reporter of *alx* was unaffected by the added $MnCl_2$ and displayed high reporter activity throughout (Fig. 1D), suggesting that PRE tunes *alx* expression post-transcriptionally in an [Mn^{2+}]-responsive manner. The response of *alx* and *mntP* to alkaline pH or added Mn^{2+} is also observed in MG1655 strain background, albeit not as pronounced as in MC4100 (Fig. S2).

We next tested the combined effect of alkaline pH and high extracellular [Mn^{2+}], on *alx* and *mntP* translational reporters. We found that *alx* and *mntP* translational reporters were induced 86- and 16-fold, respectively, in alkaline media with 500 µM $MnCl_2$ (Fig. 1E). Altogether, our results (Fig. 1B, D and E) demonstrate that the effects of elevated extracellular [Mn^{2+}] and alkaline pH on *alx* expression are additive and may enhance *alx* expression by independent routes. The *mntP* expression is induced further if both alkaline pH and extra $MnCl_2$ are provided compared to $MnCl_2$ supplementation alone (Fig. 1E) even though alkaline pH alone had no impact on *mntP* expression (Fig. 1A and

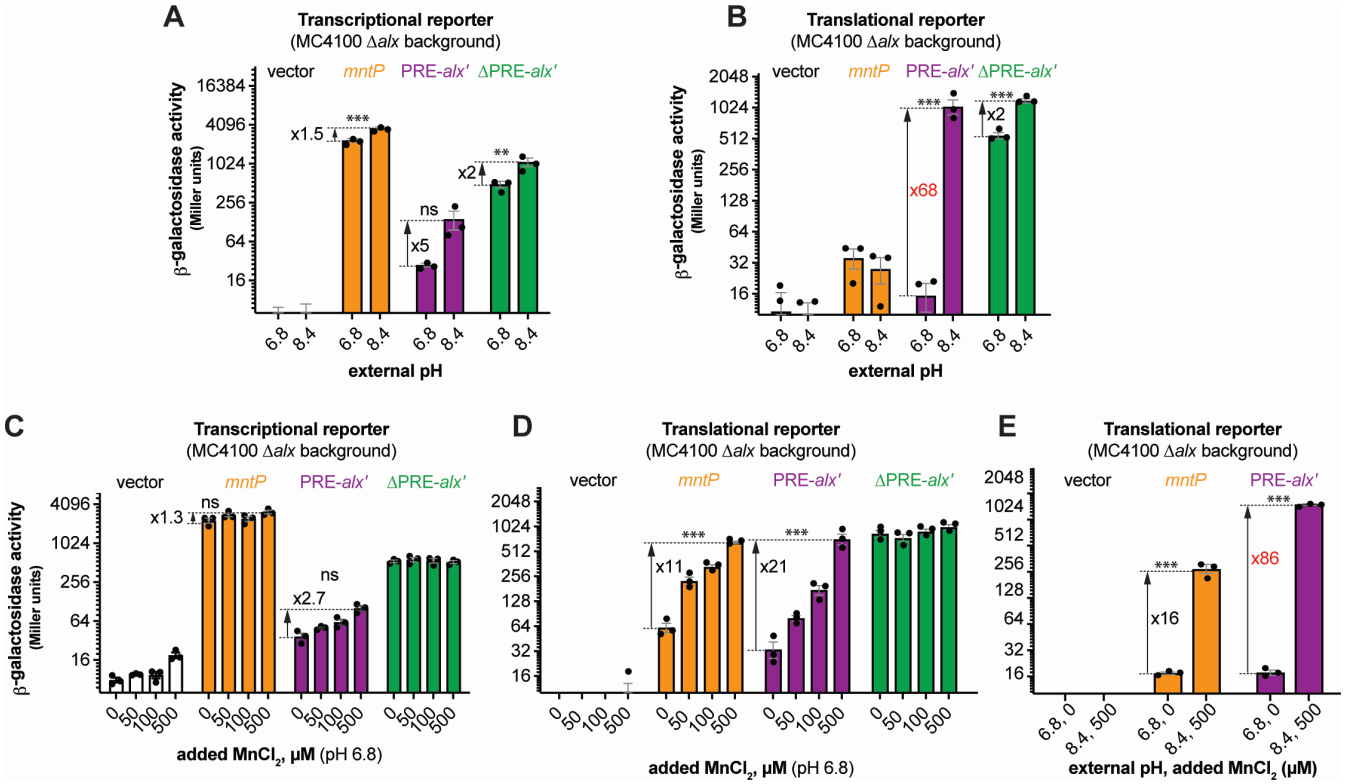

FIG 1 Regulation of *alx* expression by PRE in response to an increased external pH and [Mn^{2+}]. (A and C) β-galactosidase activities (in Miller units) of mid-log phase grown cultures of Δ*alx*::Kan derivatives of MC4100 strain of *E. coli* (RAS31) carrying one of the following plasmids: promoter-less vector with *lacZ* (pMU2385), transcriptional reporter of *mntP* (P_{mntP}-5′UTR-*mntP′-lacZ*, pRA48), transcriptional reporter of *alx* (P_{alx}-PRE-*alx′-lacZ*, pRA40), or ΔPRE derivative of *alx* transcriptional reporter (P_{alx}-alx′-*lacZ*, pRA41). The above cultures were cultivated in LBK media pH 6.8 or pH 8.4 (panel A) and LB pH 6.8 with and without supplemented $MnCl_2$ (panel C). (B and D) β-galactosidase activities of mid-log phase grown cultures of Δ*alx*::Kan derivatives of MC4100 strain of *E. coli* (RAS31) carrying one of the following plasmids: promoter-less vector with *lacZ* (pMU2386), translational reporter of *mntP* (P_{mntP}-5′UTR-*mntP′-lacZ*, pRA57), translational reporter of *alx* (P_{alx}-PRE-*alx′-lacZ*, pRA54), or ΔPRE derivative of *alx* translational reporter (P_{alx}-alx′-*lacZ*, pRA55). The above cultures were grown in LBK media pH 6.8 or 8.4 (panel B) and LB pH 6.8 with and without supplemented $MnCl_2$ (panel D). A combined effect of alkaline pH and supplemented $MnCl_2$ on translational reporters in LBK media pH 6.8 or LBK media pH 8.4 supplemented with $MnCl_2$ is illustrated in panel E. Each plotted value in a bar graph with standard error of mean (SEM) is an average of three biological replicates of the experiment. The statistical significance of the changes in the reporter signal with growth conditions was assessed by two-way ANOVA ($^{ns}P > 0.05$, $^{**}P < 0.01$, $^{***}P < 0.001$).

B). Alkaline pH, thus, enhances the Mn^{2+} effect on *mntP* expression, consistent with a previously published study (20).

The expression of *alx* is post-transcriptionally autoregulated by Mn^{2+} in alkaline pH

The *alx* translational reporter activity significantly increased at alkaline pH in the Δ*alx* strain (Fig. 1B). Intriguingly, this induction was reverted by (i) expressing Alx from a synthetic *trc* promoter (P_{trc}) in the Δ*alx* strain (Fig. 2A) or (ii) preserving the chromosomally encoded Alx (Fig. 2B). Similarly, induction of *alx* translation dropped from 21-fold (Fig. 1D) to 11-fold in a strain expressing Alx chromosomally from its native promoter in LB (pH 6.8) with 500 µM $MnCl_2$ (Fig. S3A). Alx, thus, represses its own expression post-transcriptionally at alkaline pH or high [Mn^{2+}]. This repression could be explained by Alx exporting Mn^{2+} and reducing intracellular [Mn] as described later (see "Alx mediates the export of Mn^{2+} in alkaline environment" section).

To probe if import of trace extracellular Mn^{2+} is sufficient to upregulate *alx* expression, we tested the effect of P_{trc}-expressed MntH (Mn^{2+} importer) on *alx* expression. These measurements were performed in a strain that lacks both chromosomally encoded

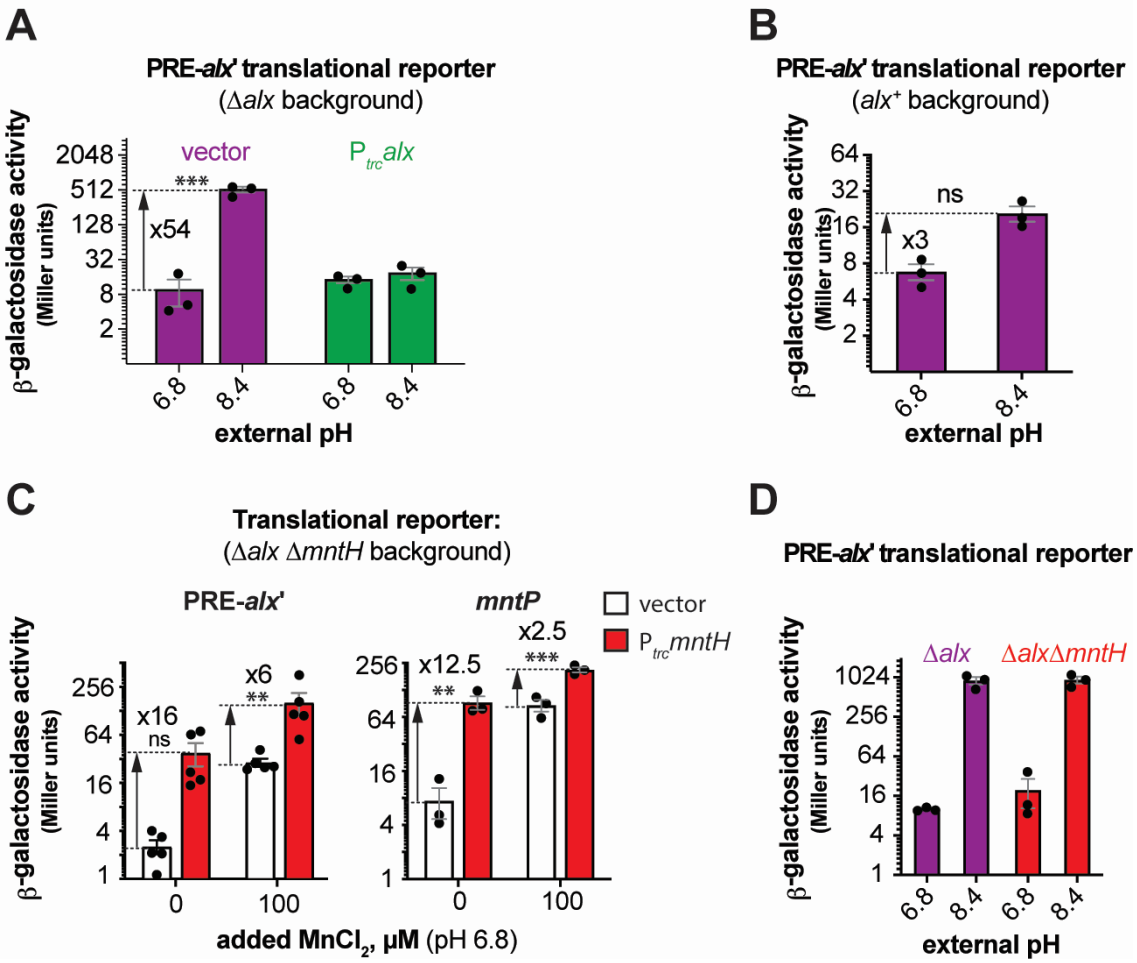

FIG 2 The induction of *alx* expression in alkaline pH and its dependence on [Mn^{2+}]. (A and B) β-galactosidase activity (in Miller units) as a reporter of *alx* translation (P_{alx}-PRE-*alx′-lacZ,* pRA54). (A) The reporter activity was measured in mid-log phase grown cultures of Δ*alx*::Kan derivative (RAS31) bearing an empty vector (pHYD5001) or pHYD5001 expressing Alx from P_{trc} promoter (pRA27). The cultures were grown in LBK media pH 6.8 or 8.4, supplemented with appropriate concentration of ampicillin, $MnCl_2$, and IPTG. (B) The reporter activity was measured in mid-log phase grown cultures of *alx*$^+$ strain (MC4100) in LBK media pH 6.8 or 8.4. (C) β-galactosidase activity (in Miller units) as a reporter of *alx* translation (P_{alx}-PRE-*alx′-lacZ,* pRA54) and *mntP* translation (P_{mntP}-5′UTR-*mntP′-lacZ,* pRA57) was measured in mid-log phase grown cultures of Δ*alx* Δ*mntH*::Kan derivative (RAS93) containing vector (pHYD5001) or derivative of pHYD5001 expressing MntH (pRA94) from P_{trc} promoter. The cells were cultured in LB pH 6.8 supplemented with appropriate concentration of ampicillin. The statistical significance of the changes in measurements was assessed by two-way ANOVA ($^{ns}P > 0.05$, $^{**}P < 0.01$, $^{***}P < 0.001$). (D) β-galactosidase activity (in Miller units) as a reporter of *alx* translation (P_{alx}-PRE-*alx′-lacZ,* pRA54) was measured in mid-log phase grown cultures of Δ*alx* mutant (RAS40) and its Δ*mntH*::Kan derivative (RAS93) in LBK media with pH 6.8 or 8.4. Each plotted value in a bar graph with standard error of mean (SEM) is an average of three biological replicates of the experiment.

Alx and MntH (Δ*alx* Δ*mntH*) in LB (pH 6.8) with and without additional $MnCl_2$. When transcribed from P_{trc}, the *mntH* expression is no longer repressed by MntR in a [Mn^{2+}]-dependent manner like chromosomal *mntH* (3); therefore, MntH should be continuously expressed from P_{trc} to import Mn^{2+} regardless of the changes in intracellular [Mn^{2+}]. Basal expression of *mntH* (no added IPTG) from P_{trc} enhanced translation of both *alx and mntP* even without added $MnCl_2$ (Fig. 2C), pointing to an MntH-mediated import of trace Mn^{2+} from the media at neutral pH and confirming that the import of extra Mn^{2+} increases *alx* expression. IPTG-induced expression of *mntH* was toxic for growth and prevented us from expression measurements in LB containing IPTG.

One possible mechanism by which alkaline pH may increase the intracellular Mn pool via trace Mn^{2+} import, thereby increasing *alx* translation, is by directly enhancing the activity of MntH importer. To address this possibility, we measured the *alx* translational reporter activity in the Δ*alx* Δ*mntH* strain. The absence of chromosomal *mntH* had no impact on the pH-induced increase in the activity of *alx* translation reporter (Fig. 2D), indicating that pH-driven induction of *alx* translation is independent of Mn^{2+} uptake by MntH at alkaline pH and suggesting an MntH-independent route for Mn^{2+} uptake operating at alkaline pH. At neutral pH, supplemental $MnCl_2$ increased *alx* translation whether or not the chromosomal *mntH* was present (Fig. S3B); thus, an alternative, MntH-independent route for Mn^{2+} into the cell likely exists regardless of pH.

Alx does not participate in maintaining cellular pH

Our data confirm earlier work which demonstrated that the expression of *alx* is induced in media with alkaline pH or high [Mn^{2+}] [Fig. 1 (19, 20, 23, 24)]. Perhaps, the simplest explanation for the pH stress-induced production of Alx would be its direct involvement in bringing the high intracellular pH back into its neutral physiological range. To probe the contribution of Alx to pH homeostasis, we tested the growth of the parent strain (MC4100) and its Δ*alx* derivative in LBK media at pH 6.8 or 8.4. The growth of the Δ*mntP* and the Δ*alx* Δ*mntP* mutants was also tested under these conditions. In general, the growth slowed in the pH 8.4 media compared to pH 6.8 (Fig. 3A). Absence of Alx did not affect the growth rate in alkaline pH in comparison to its parent strain, suggesting that Alx does not provide a growth advantage in alkaline pH.

To further rule out the involvement of Alx in pH homeostasis, cytoplasmic pH of the parent strain and its Δ*alx* derivative were measured over a range of pH values (7, 7.5, 8.5, 9, and 9.5) using genetically encoded ratiometric pHluorin as a reporter (28). Due to interference of LB broth components with the measurements, experiments were performed in M63A media. The cytoplasmic pH of the parent strain increased with an increasing external pH (Fig. 3B), consistent with prior data that showed cytoplasmic pH of *E. coli* alkalinizing in response to an increased external pH in LB and then recovering partially to 7.8 (29). The cytoplasmic pH of the Δ*alx* mutant did not differ from its parent strain across the tested pH (Fig. 3B). These results indicate that Alx participation in countering alkalization of cytoplasmic pH is unlikely.

Connection between oxidative stress and Mn^{2+} export

In line with Mn^{2+} protecting cells from oxidative damage, the expression of *mntH* (Mn^{2+} importer) increases in the presence of high extracellular or endogenously produced H_2O_2 (2, 10, 30). MntH becomes vital for growth in aerobic conditions of a strain (Δ*katG* Δ*katE* Δ*ahpCF*) lacking catalase and peroxidases that would normally clear accumulating H_2O_2 (2). The *ahpCF,* in particular, encodes a primary scavenger of endogenously produced H_2O_2 (31).

To test the role of Alx in the connection between Mn^{2+} metabolism and oxidative stress, *alx* and *mntP* were expressed from P_{trc} in the wild-type strain, its Δ*mntH,* Δ*ahpCF*, and Δ*ahpCF* Δ*mntH* derivatives at 37 or 42°C (Fig. 3C; Fig. S4A and B). We first confirmed that the Δ*ahpCF* Δ*mntH* double mutant experiences oxidative stress even upon *alx* or *mntP* expression using *katG* (bifunctional catalase-peroxidase) transcriptional reporter, which is induced in the oxidative environment (32) (Fig. S4C and D). The P_{trc}-expressed Alx and MntP only mildly affected the growth of the wild-type strain or its Δ*mntH* derivative at either temperature (Fig. S4B). In contrast, the growth of Δ*ahpCF* mutant was significantly inhibited by *mntP* expression at both temperatures (Fig. S4A). The growth inhibition became exacerbated in the Δ*ahpCF* Δ*mntH* double mutant at 42 vs 37°C (Fig. 3C), likely due to thermal effects on protein folding and function at higher temperatures (33–35). Supplemental $MnCl_2$ did not improve the growth of Δ*ahpCF* Δ*mntH* strain in the presence of P_{trc}-expressed MntP (Fig. 3C), consistent with the lack of MntH importer. The growth of Δ*ahpCF* strain was likewise unaffected by added $MnCl_2$ (Fig. S4A), suggesting that any extra Mn^{2+} imported by MntH was exported by overexpressed MntP. The

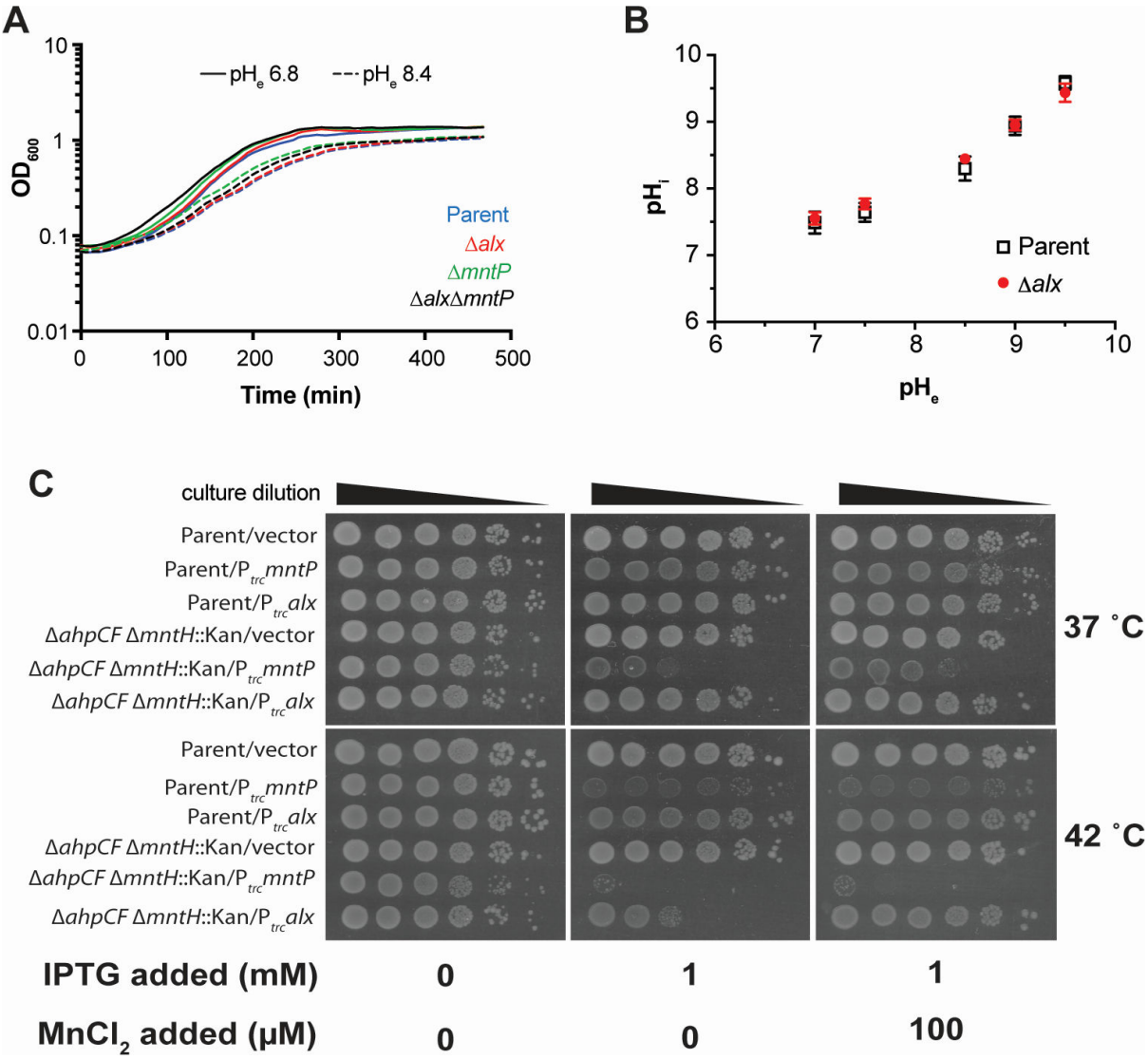

FIG 3 Effect of an increased external pH and combined effect of oxidative stress and perturbed cellular manganese levels on cellular growth. (A) Growth of the parent strain (MC4100) and its derivatives (Δ*alx*::Kan derivative, RAS31; Δ*mntP*::Kan derivative, RAS32, and Δ*alx* Δ*mntP*::Kan derivative, RAS42) in LBK media pH 6.8 or pH 8.4. (B) Cytoplasmic pH (pH_i) measured in the parent strain (MC4100) and its Δ*alx*::Kan derivative (RAS31) expressing pHluorin in M63A media of varying pH. Each plotted value of pH_i in the graph with SEM is an average of three biological replicates of the experiment. (C) The spotting assay of tenfold serial dilutions (left to right) of overnight-grown cultures of parent strain (MC4100) and its Δ*ahpCF* Δ*mntH*::Kan derivative (RAS95) each bearing an empty vector (pHYD5001) or the same vector expressing MntP (pRA29) or Alx (pRA27) from P_{trc} promoter. The serial dilutions were spotted on the surface of LB agar containing the appropriate concentration of ampicillin, $MnCl_2$, and IPTG. Plates were imaged after an incubation at 37 or 42°C for 14 hours. The data shown are representative of three biological replicates of the experiment.

P_{trc}-expressed Alx did not inhibit the growth of Δ*ahpCF* mutant at either temperature (Fig. S4A). Interestingly, however, *alx* expression inhibited the growth of Δ*ahpCF* Δ*mntH* double mutant at 42°C (Fig. 3C), serving as the first indication of a role for Alx in Mn^{2+} export. $MnCl_2$ supplementation in the presence of P_{trc}-expressed Alx rescued Δ*ahpCF* Δ*mntH* double mutant's growth (Fig. 3C), in line with the weaker Mn^{2+} export activity of Alx vs MntP suggested by other data in this work (e.g., Fig. 4D).

Previously, it was noted that *alx* expression is sensitive to the presence of an oxidizing agent, paraquat (36). Considering that *alx* expression is induced by alkaline pH, we investigated the connection between alkaline pH and oxidative stress. We assessed the oxidative stress in the parent strain and its Δ*alx* mutant in alkaline pH and in the presence

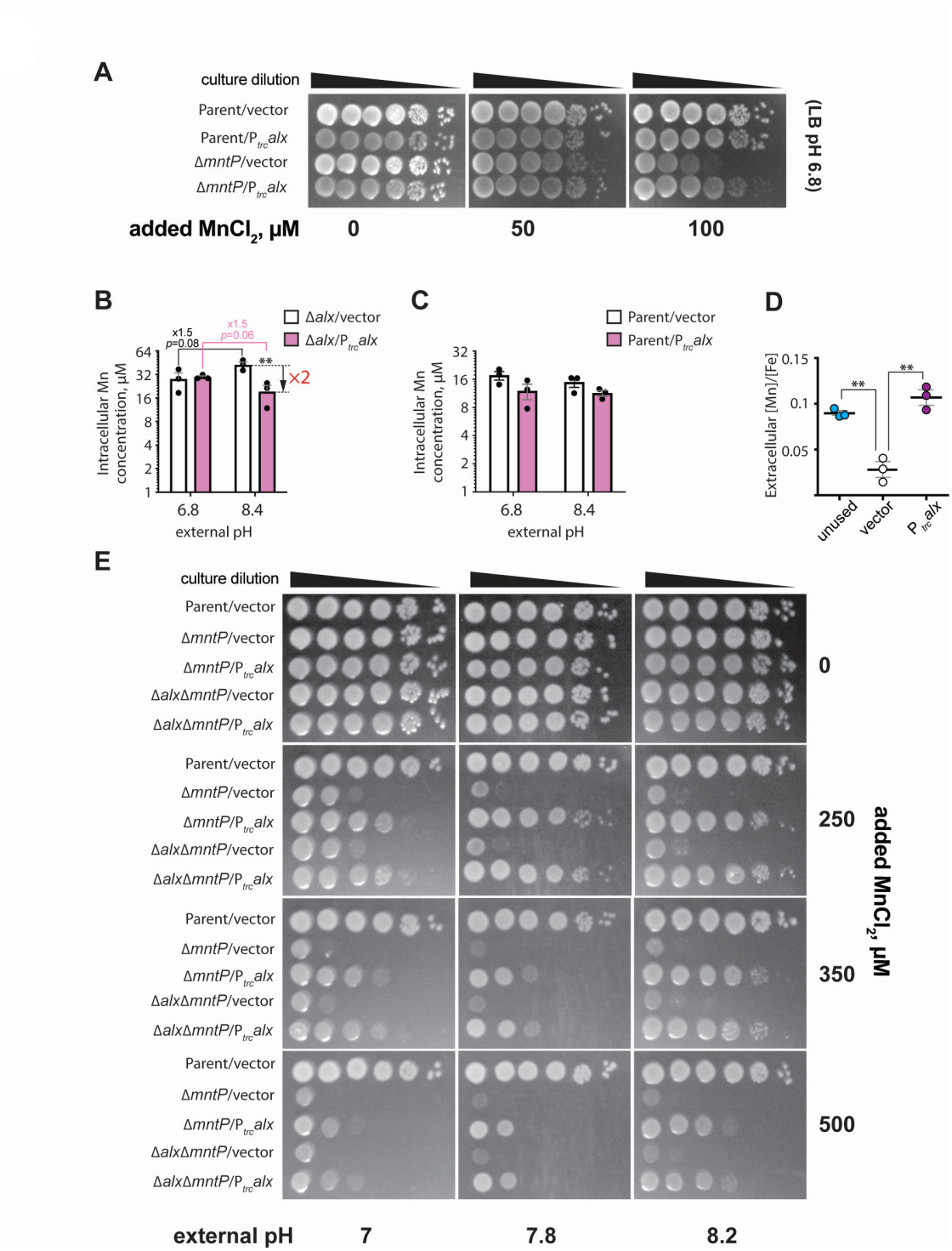

FIG 4 Alx exports Mn^{2+} at alkaline pH. (A) The spotting assay of tenfold serial dilutions (left to right) of overnight-grown cultures of parent strain (MC4100) and its Δ*mntP*::Kan derivative (RAS32), each bearing an empty vector (pHYD5001) or the same vector expressing Alx from P_{trc} promoter. The serial dilutions were spotted on the surface of LB agar containing the appropriate concentration of ampicillin, $MnCl_2$, and IPTG. The data shown are representative of three biological replicates of the experiment. Intracellular Mn concentrations measured by ICP-MS in Δ*alx* mutant (RAS31) (B) or its parent strain (MC4100) (C) carrying a vector (pHYD5001) or a derivative of pHYD5001 expressing Alx from P_{trc} promoter (pRA27). The cells were grown to mid-log phase in LBK media pH 6.8 or 8.4 supplemented with 1 mM IPTG and appropriate concentration of ampicillin. The reported metal concentrations with SEM are an average of three biological replicates of the experiment. The statistical significance of the changes in measurements was determined by two-way ANOVA (**$P < 0.01$). (D) The ratio of extracellular [Mn] to [Fe] measured by ICP-MS in unused LBK media pH 8.4 and in LBK media pH 8.4 after the exponential growth of Δ*alx* mutant (RAS31)

(Continued on next page)

FIG 4 (Continued)

containing a vector (pHYD5001) or a derivative of pHYD5001 expressing Alx from P_{trc} promoter (pRA27). The reported [Mn]/[Fe] values with SEM are an average of three biological replicates of the experiment. For unused media, reported [Mn]/[Fe] is an average of three technical replicates. The statistical significance of the changes in measurements was assessed by unpaired Student's *t* test (**$P < 0.01$). (E) The spotting assay of 10-fold serial dilutions (left to right) of overnight-grown cultures of parent strain (MC4100) and its derivatives (Δ*mntP*::Kan derivative, RAS32, and Δ*alx* Δ*mntP*::Kan derivative, RAS42), each bearing an empty vector (pHYD5001) or the same vector expressing Alx from P_{trc} promoter. The serial dilutions were spotted on the surface of LB agar of varying pH and supplemented with appropriate concentration of ampicillin, $MnCl_2$, and IPTG. The data shown are representative of three biological replicates of the experiment.

of high extracellular [Mn^{2+}], using *katG* transcriptional reporter (32). We measured the *katG* transcriptional reporter activity in LBK media with pH 6.8 or 8.4 (Fig. S4D). A marginal induction of the *katG* transcription reporter was observed in both parent and its Δ*alx* derivative at pH 8.4. The *katG* transcriptional reporter activity was marginally repressed in both parent strain and Δ*alx* mutant in LB (pH 6.8) media upon supplementation of $MnCl_2$ (Fig. S4E). Overall, these results suggest that Alx may not be directly participating in the maintenance of a redox stress at alkaline pH or high extracellular [Mn^{2+}].

Alx mediates the export of Mn^{2+} in alkaline environment

Alx exports excess Mn^{2+}

The absence of Alx alone did not alter the growth of the wild-type strain or its Δ*mntP* derivative in media with high [Mn^{2+}] (Table S4). Nonetheless, in light of both *alx* and *mntP* expression upregulated by high [Mn^{2+}] [Fig. 1D (19, 20)], we set out to test whether heterologous expression of *alx* would rescue the Mn^{2+} sensitivity phenotype of the Δ*mntP* mutant (RAS32 strain). We found that the expression of *alx* from P_{trc} (no riboswitch control), indeed, partially rescued the growth of Δ*mntP* mutant in the presence of supplemental Mn^{2+} (Fig. 4A), whereas the growth of the parent strain was not altered. These results indicate that Alx may mediate the export of Mn^{2+} in circumstances when cytoplasmic Mn^{2+} levels are elevated.

To test whether the Mn content of the cells increases at alkaline pH when Alx is most expressed, intracellular concentrations of transition metals ions (Mn, Fe, and Zn) were measured by ICP-MS in the Δ*alx* mutant (to preclude potential transport of metal ions by the Alx prior to the measurement) under neutral or alkaline pH (Fig. 4B; Fig. S5). Our measured metal ion concentrations agree with previously published values (4–6). A slight increase (1.5-fold) in the total intracellular Mn (from 28 to 42 µM) in the Δ*alx* mutant was, indeed, noted at pH 8.4 vs 6.8 (Fig. 4B). However, we did not notice an increase in the total intracellular Mn in the parent strain at pH 8.4 vs 6.8 (Fig. 4C). Importantly, we observed that although P_{trc}-expressed Alx did not change Mn levels in the Δ*alx* mutant at pH 6.8, it did reduce the total intracellular Mn 2-fold at pH 8.4 from 42 to 19 µM. In contrast, the total intracellular Mn in the parent strain did not significantly decrease with P_{trc}-expressed Alx at pH 6.8 or 8.4 (Fig. 4C). The total intracellular iron (Fe) of the Δ*alx* mutant increased 2-fold at pH 8.4 vs 6.8, whereas total intracellular zinc (Zn) remained the same at the two tested pH values (Fig. S5). Total intracellular Fe and Zn did not change with P_{trc}-expressed Alx. These results suggest that Alx may selectively prevent the buildup of intracellular Mn specifically under alkaline pH.

To corroborate the intracellular metal ion analysis, we quantified metal ions (specifically Mn and Fe) in the spent media by ICP-MS (Fig. 4D). The [Mn]/[Fe] ratio is often used as a measure of intracellular Mn in bacterial pathogens (37–39); here, we employed this ratio to assess the changes in extracellular [Mn]. Notably, the Δ*alx* strain grown in LBK pH 8.4 media exhibited a statistically significant reduction in the media [Mn]/[Fe] compared to unused LBK (Fig. 4D). If Alx were to export Mn^{2+} at alkaline pH, then spent media Mn would be expected to increase upon P_{trc}-driven Alx expression, thus increasing the [Mn]/[Fe]. The P_{trc}-expressed Alx in the Δ*alx* strain, indeed, restored the [Mn]/[Fe] in LBK pH 8.4 media. These results collectively provide evidence for Alx exporting Mn^{2+} at alkaline pH.

Alx Mn^{2+} export activity is stimulated by alkaline pH

The P_{trc}-driven expression of Alx decreases intracellular [Mn] in the Δ*alx* mutant at pH 8.4, but not pH 6.8, suggesting that Mn^{2+} transport by Alx is pH-dependent (Fig. 4B). To test the possibility that the mechanism of Mn^{2+} export by Alx is proton dependent, we performed assays for detecting substrate-induced proton release in inside-out vesicles using published procedures (40). Everted membrane vesicles were prepared with the Δ*alx* Δ*mntP* double mutant containing an empty vector or a vector expressing a human influenza hemagglutinin (HA)-tagged derivative of Alx or MntP (Alx^{HA} or $MntP^{HA}$). Successful expression of each tagged protein was confirmed by anti-HA immunoblotting. A pH gradient across the vesicle membrane was generated via F_0F_1 ATPase activity by the addition of ATP to the vesicle suspension (Fig. S6). To monitor the generation of pH gradient, a pH gradient-sensitive, fluorescent dye 9-amino-6-chloro-2-methoxyacridine (ACMA) was employed. An expected quenching of fluorescence occurred upon the addition of ATP, suggesting vesicles were active. If Mn^{2+} transport by Alx or MntP were dependent on proton release, then a dequenching of ACMA fluorescence upon the addition of $MnCl_2$ would be expected. However, we did not observe a significant change in the fluorescence intensity of ACMA upon the addition of $MnCl_2$ (Fig. S6C and D), suggesting that the transport of Mn^{2+} by Alx and MntP is unlikely to be accompanied by an H^+ antiport.

We speculated that alkaline pH may, thus, stimulate the Mn^{2+} export activity of Alx directly, perhaps by altering the protonation state of key Alx residues (see "A set of acidic residues in the transmembrane helices are critical for Alx-mediated Mn^{2+} export" section of the Results). To test this hypothesis, we probed the combined effect of elevated pH and extracellular [Mn^{2+}] on the Mn^{2+} sensitivity phenotype of the Δ*mntP* mutant (Fig. 4E). The Mn^{2+} sensitivity of the Δ*mntP* mutant was exacerbated by the increasing concentration of $MnCl_2$ in the media or increasing the media pH. This is expected since increasing media [Mn^{2+}] correlates with an increase in the cytoplasmic [Mn] in the Δ*mntP* mutant (4, 13), and alkalinization of the media likewise increases cytoplasmic [Mn] (Fig. 4B), altogether leading to Mn toxicity. We noted a pH-dependent boost in the ability of P_{trc}-expressed Alx to rescue the growth of the Δ*mntP* mutant in media with increasing [Mn^{2+}] (Fig. 4E), supporting the notion that the Mn^{2+} export activity of Alx is stimulated by alkaline pH. Alx appears to be a low-activity Mn^{2+} exporter, in contrast to MntP, because its rescue ability dropped off at particularly high extracellular [Mn^{2+}] (see 350 and 500 µM $MnCl_2$ panels). The growth of the Δ*alx* Δ*mntP* strain closely resembled that of the Δ*mntP* mutant at elevated media [Mn^{2+}] and pH (Fig. 4E). Likewise, the rescue of the growth of the Δ*alx* Δ*mntP* double mutant by overexpressed Alx was similar to that in the Δ*mntP* mutant (Fig. 4E). These observations suggest that chromosomally encoded Alx mitigates the mild perturbations in Mn^{2+} levels brought about by alkaline pH, and its Mn^{2+} export activity appears to be milder compared to the chromosomally encoded MntP.

A set of acidic residues in the transmembrane helices is critical for Mn^{2+} export by Alx

Currently, no experimental three-dimensional (3D) structural information for either Alx or MntP exists. To glean some insight into Alx architecture, its two-dimensional (2D) topology was predicted with multiple web-based tools listed in Table S5. This prediction identified nine Alx transmembrane segments (TMS1-9, Fig. 5A; Table S5), with an overall N-out (periplasmic) and C-in (cytoplasmic) Alx topology. Regardless of the prediction tool used, we noted the presence of acidic residues in the TMS, which is unusual and may suggest the functional importance of these side chains, as demonstrated previously for the export of Mn^{2+} by MntP (14). Two of these residues (D92 and D222) are conserved across members of the TerC family to which Alx belongs (14). Similar to topology-predicted arrangement, Alx displayed an N-out C-in conformation in the 3D structure predicted by the AlphaFold server (Fig. 5B).

To probe the importance of the acidic residues predicted to be in the TMS of Alx, the effect of P_{trc}-expressed HA-tagged Alx bearing conservative (D to N or E to Q) replacements was tested on the growth of the Δ*mntP* mutant in LB media with neutral or alkaline pH and added $MnCl_2$ (Fig. 5; Fig. S7). With this strategy, the expression of the wild-type HA-tagged Alx rescued the growth of the Δ*mntP* mutant like the tag-less version of Alx, suggesting that the HA tag did not alter the activity of Alx. The P_{trc}-expressed Alx bearing E86Q, D92N, E213Q, D216N, or D222N replacement (denoted as Alx^{HA}_{E86Q}, Alx^{HA}_{D92N}, Alx^{HA}_{E213Q}, Alx^{HA}_{D216N}, or Alx^{HA}_{D222N}, respectively) did not rescue the growth of the Δ*mntP* strain in media supplemented with $MnCl_2$, whereas Alx bearing

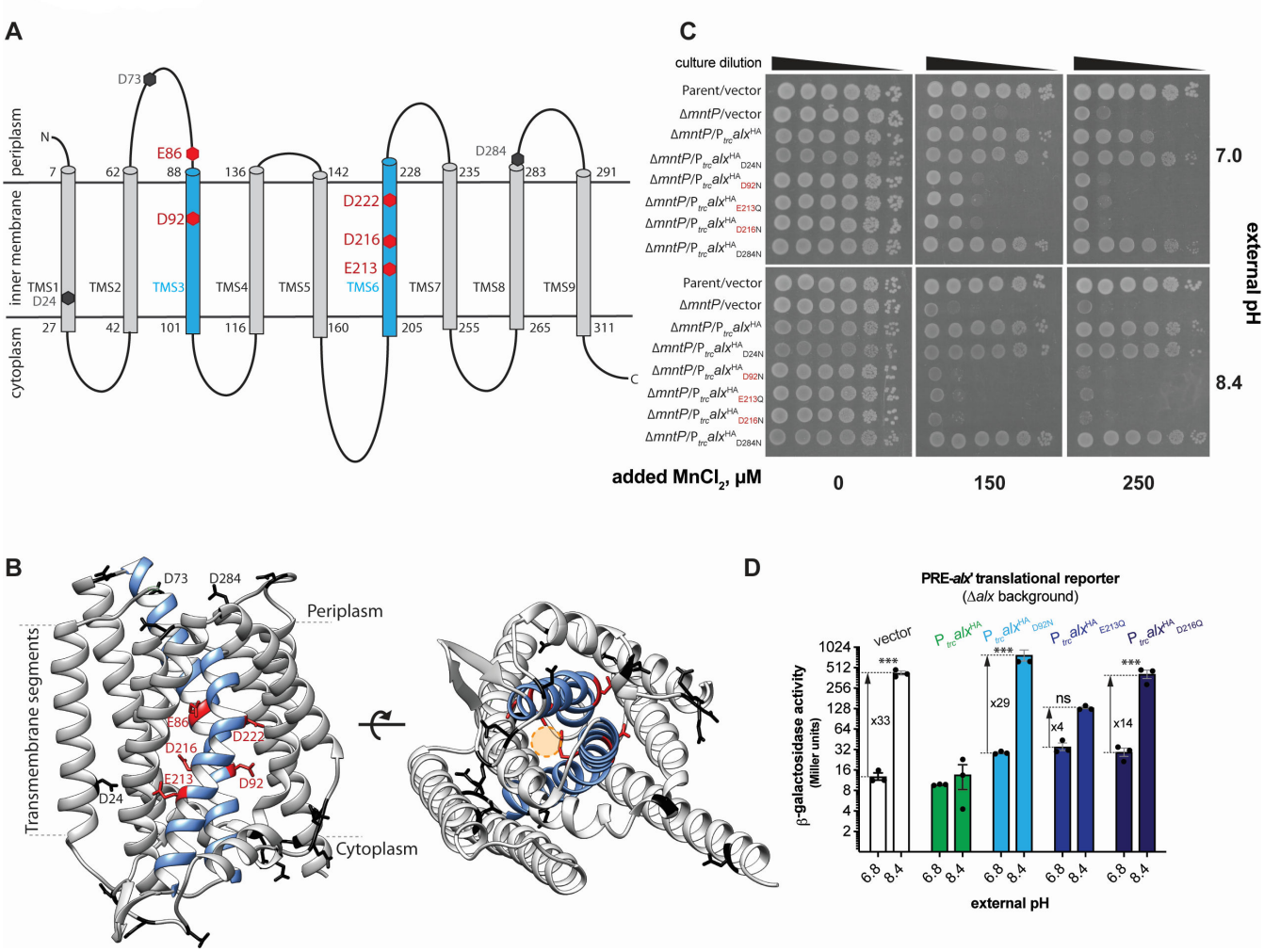

FIG 5 Structural model of Alx and functional relevance of its acidic residues in Mn^{2+} export. (A) The 2D topological model of Alx predicted with DeepTMHMM algorithm and relative positions of acidic residues in transmembrane segments (TMS). (B) AlphaFold-predicted 3D structure of Alx and relative positions acidic residues in TMS. A hypothetical channel for the export of Mn^{2+} is displayed as a circle in the predicted structure. (C) The spotting assay of tenfold serial dilutions (left to right) of overnight-grown cultures of parent strain (MC4100) bearing an empty vector (pHYD5001) and Δ*mntP*::Kan mutant (RAS32) bearing one of the following plasmids: a vector (pHYD5001), a derivative of pHYD5001 expressing Alx from P_{trc} promoter (pRA27), a derivative of pHYD5001 expressing Alx^{HA} from a P_{trc} promoter (pRA50), a derivative of pRA50 expressing Alx^{HA}_{D24N} (pRA61), Alx^{HA}_{D92N} (pRA62), Alx^{HA}_{E213Q} (pRA63), Alx^{HA}_{D216N} (pRA64), and Alx^{HA}_{D284N} (pRA58). The serial dilutions were spotted on the surface of LB agar of varying pH and supplemented with appropriate concentration of ampicillin, $MnCl_2$, and IPTG. The data shown are representative of three biological replicates of the experiment. (D) β-galactosidase activity (in Miller units) as a reporter of *alx* translation (P_{alx}-PRE-*alx'-lacZ,* pRA54) was measured in mid-log phase grown cultures of Δ*alx*::Kan strain (RAS31) bearing vector (pHYD5001) and a derivative of pHYD5001 expressing Alx^{HA} (pRA27), Alx^{HA}_{D92N} (pRA62), Alx^{HA}_{E213Q} (pRA63), Alx^{HA}_{D216N} (pRA64) from P_{trc} promoter. The cultures were grown in LBK media pH 6.8 or 8.4, supplemented with appropriate concentration of ampicillin and 1 mM IPTG. Each plotted value in a bar graph with standard error of mean (SEM) is an average of three biological replicates of the experiment. The statistical significance of changes in the reporter activity was assessed by two-way ANOVA ($^{ns}P > 0.05$, $^{*}P < 0.05$, $^{**}P < 0.01$, $^{***}P < 0.001$).

D24N, D73N, or D284N substitution did so (Fig. 5C; Fig. S8). The expression of HA-tagged Alx mutants was unchanged compared to the wild-type Alx (Fig. S8), ruling out Alx expression defects as a cause for the failure to rescue the Δ*mntP* mutant. These results indicated that E86, D92, E213, D216, and D222 are important for Alx-mediated Mn^{2+} export.

To expand upon the functional role of inner membrane acidic residues in the Alx protein, we performed a suite of *alx* translational reporter experiments. Our prior reporter assays demonstrated that Alx displays negative autoregulation, since a translational reporter of *alx* was not induced by alkaline pH or high [Mn^{2+}] if Alx was expressed from P_{trc}, presumably because of Alx-mediated Mn^{2+} export (Fig. 1D and 2A; Fig. S3A). We, thus, took advantage of this behavior and employed Alx mutants defective in Mn^{2+} export to link the effects of alkaline pH and [Mn^{2+}] on *alx* expression. Specifically, we tested the impact of P_{trc}-expressed Alx^{HA}_{D92N}, Alx^{HA}_{E213Q}, and Alx^{HA}_{D216N} on *alx* translational reporter activity in LBK pH 6.8 or 8.4 (Fig. 5D). The expression of wild-type Alx^{HA} from a plasmid repressed the activity of *alx* translational reporter at alkaline pH in the Δ*alx* strain (RAS31) as expected. The reason behind the lower (33- vs 68-fold) pH-induced increase in *alx* translation in this experiment (strain co-transformed with the translational reporter and Alx expression vector) vs earlier experiment (Fig. 1B, strain transformed with translational reporter only) is unclear. Nevertheless, the expression of either Alx^{HA}_{D92N}, Alx^{HA}_{E213Q}, or Alx^{HA}_{D216N} did *not* repress *alx* translational reporter activity as wild-type Alx^{HA} did. The fold induction of *alx* translational reporter activity varied (29, 4, and 14 for Alx^{HA}_{D92N}, Alx^{HA}_{E213Q}, and Alx^{HA}_{D216N}, respectively), indicating that Alx^{HA}_{E213Q} and Alx^{HA}_{D216N} retain partial activity, whereas Alx^{HA}_{D92N} is inactive. Overall, negative autoregulation of *alx* expression in response to alkaline pH is no longer observed when Alx mutants defective in Mn^{2+} transport are expressed; in other words, *alx* expression stays "on." This suggests a connection between the induction of *alx* expression and Alx-mediated export of Mn^{2+} in alkaline pH, where the return of intracellular [Mn^{2+}] back to its "healthy" levels via Alx export shuts down further production of Alx.

DISCUSSION

In this work, we investigated in depth the effect of increased extracellular pH and [Mn^{2+}] on *alx* expression and provided multiple pieces of evidence for Alx export of Mn^{2+} upon alkalinization of the cytoplasm. Our results corroborate earlier findings that *alx* expression is upregulated by both alkaline pH and elevated [Mn^{2+}] (19, 20, 23, 24, 41) in a riboswitch-dependent manner (Fig. 1). We confirmed that the cytoplasm, indeed, alkalinizes when cells are grown in alkaline media (Fig. 3B); therefore, our observed changes in gene expression and intracellular metal ion content are a consequence of alkaline cytoplasmic pH. The absence of Alx had no impact on cytoplasmic alkalinization with increasing media pH (Fig. 3B) and did not affect cellular growth in alkaline media (Fig. 3A), ruling out direct Alx involvement in pH homeostasis. The expression of Alx did, however, lower total intracellular [Mn], but only at alkaline pH (Fig. 4B), thus implicating Alx as a Mn^{2+} exporter in alkaline pH. With this newly uncovered function of Alx, our work points to a connection between the two environmental cues: alkaline pH and elevated [Mn^{2+}]. A recent study demonstrated that cytosol alkalinizes in the presence of excess extracellular Mn^{2+} due to increased ammonia production within an *E. coli* cell (20); here, we show that the reverse is also true: an alkaline environment promotes the import of Mn^{2+} into the cell.

Intracellular pH and Mn^{2+} content are linked

We find that alkalinization of the cytoplasm leads to an increase in the intracellular [Mn]. Specifically, our intracellular metal ion measurements show a 1.5-fold increase in [Mn] at pH 8.4 vs 6.8 in the Δ*alx* strain, from 28 to 42 µM (Fig. 4B). Additional indirect data support this increase. First, the Mn^{2+} sensitivity of Δ*mntP* mutant is exacerbated at alkaline pH (Fig. 4D). Second, even though alkaline pH alone did not impact

mntP translation, a combination of alkaline pH and extra Mn^{2+} in the media led to a greater *mntP* induction than Mn^{2+} alone (16- and 11-fold, respectively, Fig. 1E). Because upregulation of *mntP* translation is directly proportional to [Mn^{2+}] (Fig. 1D), the additional increase is likely due to the additional Mn^{2+} imported into the cell at alkaline vs neutral pH. The fact that alkaline pH alone had no effect on *mntP* translation suggests that there is a threshold total intracellular [Mn] of >42 µM needed to begin producing additional MntP based on intracellular Mn measurements at alkaline pH (Fig. 4B). Third, the P_{trc}-expressed MntH, the only characterized Mn^{2+} importer in *E. coli* K12 strain, induced *alx* and *mntP* translational reporter at neutral pH (Fig. 2C). The mechanism of the alkaline pH-induced Mn^{2+} import, on the other hand, is unclear but does not involve MntH (Fig. 2D; Fig. S3B), implicating a potential alternative path for Mn^{2+} into the cell.

Why would a cell import Mn^{2+} upon cytosol alkalinization? Among the possible roles that imported Mn^{2+} could play in an alkaline cytosol is its function as a redox center in the superoxide dismutase SodA and other mononuclear metal enzymes where Mn^{2+} can replace Fe^{2+} as a cofactor to prevent protein damage from oxidative stress (1, 2, 42). It may, thus, be an adaptive strategy that cells import Mn^{2+} in response to elevated ROS in alkaline pH. The expression of MntP (Mn^{2+} exporter) and Alx slowed the aerobic growth of a sensitized strain that lacks H_2O_2 degrading enzymes (AhpCF and KatG) (14). The effects of MntP overproduction on the growth of Δ*ahpCF* Δ*katG* strain are explained by reduced intracellular [Mn^{2+}] (due to Mn^{2+} export by MntP) and corresponding reduced protection from ROS. Similar effects of Alx overproduction on this strain's growth, however, were explained differently by reference (14) as Alx was viewed as an Mn^{2+} importer. Alx export of Mn^{2+} by analogy to MntP, on the other hand, better explains the observed slower growth of the Δ*ahpCF* Δ*katG* strain upon Alx overexpression because P_{trc}-expressed Alx rescues the growth of the Δ*mntP* mutant in media with extra $Mn^{2+}$and reduces the intracellular [Mn^{2+}] in alkaline pH.

The *alx* translational reporter displayed a 68-fold induction in alkaline pH media and a 21-fold induction in neutral pH media with 500 µM $MnCl_2$, with an 86-fold induction when two environmental cues (alkalinity and high [Mn^{2+}]) were combined (Fig. 1). Alkaline pH, thus, augments the effects of elevated [Mn^{2+}] on *alx* expression. The alkaline pH-induced Mn^{2+} import also provides an alternate explanation to a recent report where increased cytoplasmic [Mn^{2+}] results in higher activation of *mntP* riboswitch upon alkalinization in media with extra Mn^{2+} in contrast to the proposed tighter interaction between Mn^{2+} and the *mntP* riboswitch element (20). Differences in the fold induction by the two cues are reflective of a potentially distinct mechanism for modulation of *alx* expression in alkaline pH that depends on elevated cytoplasmic [Mn^{2+}]. A future direction for deconvoluting the mechanism of pH and Mn^{2+} control of *alx* expression will be to examine how pH and Mn^{2+} differentially affect *alx* mRNA folding, and specifically folding of its 5′ UTR riboswitch.

Our results contradict Kalita et al.'s (20) assertion that *alx* and *mntP* riboswitches necessitate a requirement of *both* high [Mn^{2+}] and alkaline pH for their optimal activation; however, our results are supportive of the findings that *alx* riboswitch is responsive to both alkaline pH [(20, 23, 24), Fig. 1; Fig. S2] and Mn^{2+} [(19, 20), Fig. 1; Fig. S2]. Furthermore, our research supports Kalita et al.'s conclusion that the *alx* and *mntP* riboswitches require both increased levels of Mn^{2+} and an alkaline pH for their full activation.

Mn^{2+} export by Alx

A previous study proposed that Alx may function as an Mn^{2+} importer based on the cellular [Mn] measurements in the presence of supplemented Mn^{2+} (14). Contrary to this earlier study, here, we provided multiple lines of evidence for the Alx-mediated export of Mn^{2+} in alkaline pH or conditions where cytoplasmic Mn levels go up. First, the P_{trc}-expressed Alx inhibited the growth of the Δ*ahpCF* Δ*mntH*, oxidatively stressed (2, 14, 31) and Mn-limited strain at 42°C (Fig. 3C). Second, the inability of Δ*mntP* strain to grow with added Mn^{2+} was partially rescued by P_{trc}-expressed Alx (Fig. 3A). This rescue

phenotype was missed in the previous work (14) likely because rescue experiments were performed at neutral pH only. Strikingly, the rescue of Δ*mntP* mutant's sensitivity toward Mn^{2+} by P_{trc}-expressed Alx becomes more pronounced with increasing pH, while Mn^{2+} sensitivity of Δ*mntP* mutant becomes exacerbated with increasing pH (Fig. 4E). Fourth, the P_{trc}-expressed Alx in the Δ*alx* strain reduced intracellular [Mn^{2+}] ~2-fold but only in alkaline pH, returning intracellular [Mn^{2+}] from 42 to 19 µM (Fig. 4B). Therefore, improved growth of the Δ*mntP* mutant with P_{trc}-expressed Alx can be explained by the increased activity of Alx in alkaline pH.

Mn^{2+} export by Alx at alkaline pH is also supported by the observed negative feedback regulation of *alx* expression. Specifically, the alkaline induction of *alx* translation (68-fold) was repressed by the presence of Alx encoded chromosomally from a native promoter or expressed from P_{trc} (Fig. 1B, 2A and B). These results can be explained if Alx exports Mn^{2+} thereby reducing cytoplasmic [Mn^{2+}] to the levels that no longer stimulate *alx* translation. The expression of Alx chromosomally resulted in only a 2-fold reduction in *alx* translation at pH 6.8 and 500 µM added $MnCl_2$: compare Mn-induced increase in *alx* translation in Fig. S3A (11-fold) in the presence of chromosomal *alx* to Fig. 1D in the absence of chromosomal *alx* (21-fold). The mild reporter activity reduction, in this case, can be explained by the lack of alkaline pH-stimulated Mn^{2+} export activity of Alx.

The driving force and mechanism behind Alx's export of Mn^{2+} remain an open direction for future work. A proton gradient is unlikely to drive this transport because we do not observe a loss of pH gradient upon supplementation of Mn^{2+} to inverted membrane vesicles containing Alx (Fig. S6), ruling out Alx as an Mn^{2+}/H^+ antiporter. In another system, a high concentration of potassium ion (K^+) in the media was proposed to stimulate the activity of K^+ export proteins and inhibit the activity of K^+ uptake proteins (43–45). However, in the case of Alx, the stimulation of its activity by alkaline pH is unlikely through just an increase in cellular [Mn^{2+}]. This reasoning is supported by the observation that P_{trc}-expressed Alx rescues the growth of Δ*mntP* mutant at intermediate but not high media [Mn^{2+}] (Fig. 4A and E). The most likely explanation for the stimulation of Alx activity by alkaline pH could be pH-driven structural changes in the Alx protein that affect its Mn^{2+} export. We identified several acidic residues in TMS3 and TMS6 of Alx (E86, D92, E213, D126, and D222) crucial for Mn^{2+} transport, by analogy to MntP and MntH [Fig. 5B (8, 14)]. The interaction of positively charged solute (Mn^{2+}), and these acidic side chains may provide a path for Mn^{2+} transport as depicted in Fig. 5B.

Role of Alx in bacterial physiology

We did not observe a growth phenotype for the Δ*alx* mutant indicating that chromosomally encoded Alx does not provide a measurable advantage in the tested laboratory conditions of media [Mn^{2+}], pH, and chosen bacterial strain. This observation also suggests that a pH-driven increase in total intracellular [Mn] to 42 µM is not toxic to *E. coli*. Overexpression of Alx, however, did rescue the growth of the Δ*mntP* mutant in alkaline media with added Mn^{2+}, which suggests that Alx functions as a weak Mn^{2+} exporter. To draw a comparison with other bacterial species, *Bacillus subtilis* (*B. subtilis*) maintains a higher intracellular [Mn]/[Fe] compared to *E. coli* (39, 46). A conditional requirement of balancing the excess Mn^{2+} import in *B. subtilis* is achieved through transcriptional regulators that repress the expression of Mn^{2+} importers and the presence of multiple Mn^{2+} exporters (39, 47–49). Interestingly, an Alx ortholog in *B. subtilis* regulated by an Mn^{2+}-responsive riboswitch was proposed to detoxify excess Mn and metalate exoenzymes (19, 47, 50). It will be fascinating to understand the riboswitch-controlled regulation of Alx in *E. coli* that make it both pH and Mn^{2+} responsive and how it evolved in *B. subtilis*.

Curiously, an earlier study reported that *alx* is expressed at both neutral and alkaline pH during anaerobic growth of *E. coli* where ROS stress is minimal (51). Consequently, a cell no longer needs additional Mn^{2+} during anaerobic growth and preventing Mn^{2+} buildup due to its uptake becomes important. This would explain why *alx* is expressed

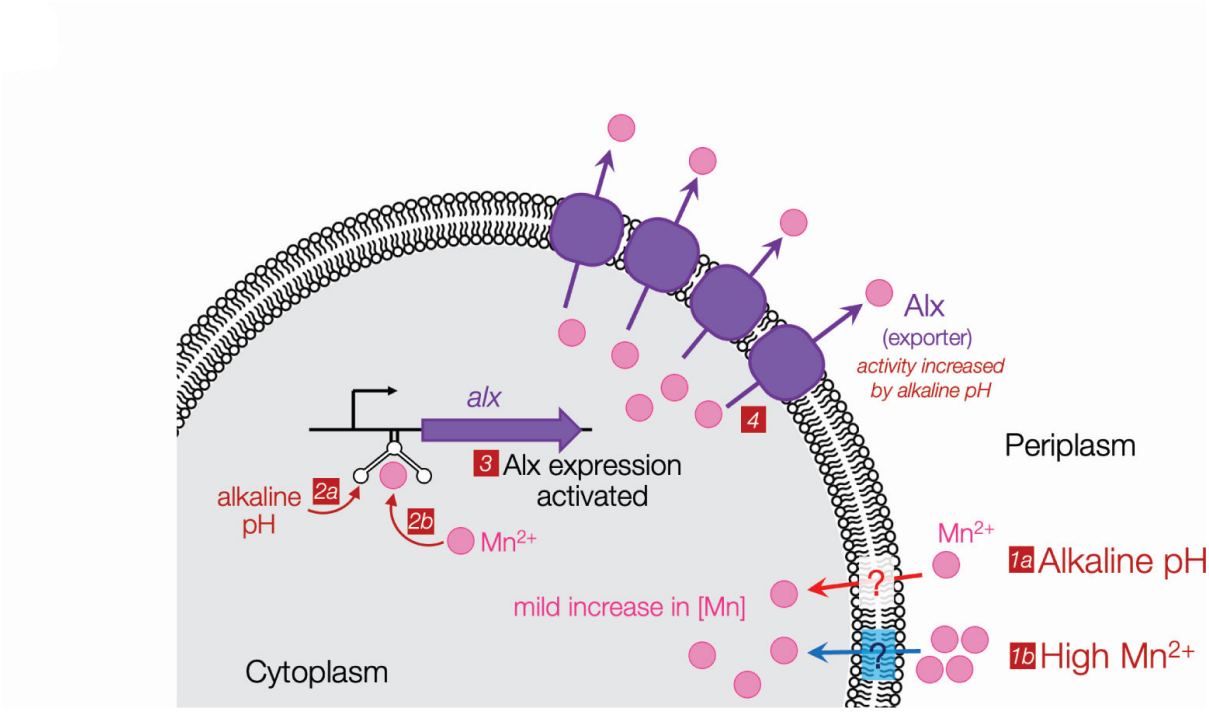

FIG 6 A model for the regulation of *alx* expression in *E. coli*. Manganese enters the cell by an uncharacterized transport mechanism through the inner membrane during growth in an alkaline environment (1a) or elevated concentration of Mn^{2+} (1b). The subtle changes in intracellular Mn level are sensed in alkaline (2a) or neutral pH (2b) by the *alx* riboswitch, triggering an increase in expression of Alx in an Mn-dependent manner (3). The export of excess Mn by Alx, stimulated by alkaline pH, restores cellular Mn levels (4).

even at neutral pH in anaerobic conditions (51). We speculate that the expression of *alx* may provide an advantage in environmental niches where *E. coli* and other enterobacteria are challenged by both alkaline pH and hypoxia, such as the portion of human gut from duodenum to ileum (52, 53). To cope with the threat of high [Mn^{2+}] in the environment, the Mn^{2+} export by chromosomally encoded MntP is sufficient to protect the cell. On the other hand, when changes in intracellular [Mn^{2+}] are mild, e.g., as brought about by alkaline pH, Alx fulfills the job of maintaining healthy levels of Mn^{2+} inside the cell (Fig. 6). We, thus, posit that Alx-mediated Mn^{2+} export provides a primary protective mechanism that fine tunes the cytoplasmic [Mn^{2+}], especially during alkaline stress.

MATERIALS AND METHODS

Chemicals

Manganese (II) chloride tetrahydrate and potassium benzoate were purchased from Alfa Aesar. Tris(hydroxymethyl)methyl-3-amino propane sulfonic acid (TAPS) was purchased from Acros Organics. *N*-(1,1-dimethyl-2-hydroxyethyl)-3-amino-2-hydroxypropane sulfonic acid (AMPSO), nigericin sodium salt, and valinomycin were purchased from Sigma-Aldrich. 9-Amino-6-chloro-2-methoxyacridine (ACMA) was purchased from Invitrogen. *o*-nitrophenyl-β-D-galactopyranoside was purchased from Thermo Scientific. Isopropyl-β-D-thiogalactopyranoside (IPTG) and 3-(*N*-morpholino) propane sulfonic acid (MOPS) were purchased from Fisher Scientific.

Bacterial strain construction and growth conditions

The strains employed in this study are derivatives of *E. coli* K12 and tabulated in Table S1. The MG1655 Δ*ahpCF*::Kan strain was constructed by following the procedures

of recombineering as described in reference (54). The Δ*alx*::Kan, Δ*mntP*::Kan, and Δ*mntH*::Kan mutations were sourced from appropriate strains from the Keio collection (55) and introduced into recipient strains by P1 transduction. The gene encoding the Kanamycin resistance determinant was excised upon treatment with plasmid pCP20 in Δ*alx*::Kan (54). All strains were cultivated in LB agar or broth at 37°C. The pH of LB agar or LB broth employed in this study was 7.2 unless stated otherwise. We also employed potassium-modified LB medium (LBK), where equimolar KCl replaced NaCl, buffered with 100 mM *N*-[tris(hydroxymethyl)methyl]-3-amino propane sulfonic acid (TAPS), and pH adjusted with KOH to 8.4 (41). The pH of unbuffered LBK medium employed was 6.8. In other experiments, LB agar was buffered with HEPES, Tris-Cl, and TAPS (50 mM final concentration), and pH was adjusted to 7, 7.8, and 8.2, respectively.

Plasmid construction

The plasmid pRA40 carrying P_{alx}-PRE-*alx′* (transcriptional reporter of *alx*) was constructed by PCR-amplifying MC4100 chromosomal DNA from 473 nucleotides upstream and 53 nucleotides downstream from the translation start site of *alx* (24) using oligos RAV5 and RAV48 and then cloning the PCR product into the PstI and KpnI sites of a single-copy plasmid pMU2385. The plasmid pRA54 (translational reporter of *alx*) was constructed similarly by PCR-amplifying MC4100 chromosomal DNA from 473 nucleotides upstream and 99 nucleotides downstream from the translation start site of *alx* using oligos RAV5 and RAV23 and cloning of PCR product into the PstI and BamHI sites of single-copy plasmid pMU2386, such that the first 33 codons of the ORF are in frame with the 8th codon of *lacZ*. We extended the length of *alx′* in the translational reporter of *alx* (98 nucleotides downstream from the translation start site), compared to the transcriptional reporter (53 nucleotides downstream from the translation start site) for two reasons: (1) to include the last putative transcriptional pause proximal to the *alx* translation start site (56) that turned out being important for maximal *alx* induction and (2) to increase the probability of the Alx′-LacZ hybrid protein localizing in the cytoplasm (refer to the topological analysis of Alx in Fig. 5A). The ΔPRE derivatives of transcriptional (pRA41) and translational (pRA55) reporters of *alx* were constructed by site-directed mutagenesis of plasmids pRA40 and pRA54, respectively, using oligos RAV15 and RAV16.

The pRA48 plasmid (transcriptional reporter of *mntP*) was constructed by PCR-amplifying MC4100 chromosomal DNA from 882 nucleotides upstream and 47 nucleotides downstream from the translation start site of *mntP* (19) using oligos RAV119 and RAV120 and then cloning the PCR product into the PstI and KpnI sites of a single-copy plasmid pMU2385. The plasmid pRA57 (translational reporter of *mntP*) was constructed by PCR-amplifying MC4100 chromosomal DNA from 882 nucleotides upstream and 47 nucleotides downstream from the translation start sites of *mntP* (19) using oligos RAV119 and RAV126 and cloning of the PCR product in the PstI and SalI sites of single-copy plasmid pMU2386, such that the first 47 nucleotides of the *mntP* ORF are in frame with the 8th codon of *lacZ*.

Oligos RAV65 and RAV66 were employed to PCR-amplify the gene encoding pHluorin from a plasmid (pGFPR01) obtained from a strain JLS1105 (28). The PCR product was cloned into pHYD5001 using Gibson assembly, producing pRA46. Oligos RAV11 and RAV12 were used to PCR-amplify *alx* from the MC4100 genomic DNA. The PCR product was then cloned into the NdeI and HindIII sites of pHYD5001. The resulting pHYD5001 expressing *alx* from P_{trc} promoter was denoted as pRA27. It was noted upon sequencing of pRA27 that the NdeI site was mutated but *alx* ORF is still retained. Similarly, oligos pairs RAV13, RAV14 and RAV269, RAV270 were used to PCR-amplify *mntP* and *mntH*, respectively, from the MC4100 genomic DNA. The PCR products were cloned into the NdeI and HindIII sites of pHYD5001. The resulting pHYD5001 derivatives expressing *mntP* and *mntH* from P_{trc} promoter were denoted as pRA29 and pRA94, respectively. The pRA50 plasmid encoding the HA epitope-tagged version of Alx on N-terminus from P_{trc} promoter was constructed by PCR amplification with oligos RAV139 and RAV12 and cloning the product into the NdeI and HindIII sites of pHYD5001. Similarly, pRA70

was constructed to express the HA epitope-tagged MntP on their N-terminus from P_{trc} promoter. The PCR product was generated by using oligos RAV178 and RAV14 for amplification of *mntP* from MC4100 genomic DNA as template. PCR products were cloned into the NdeI and HindIII sites of pHYD5001. Other plasmids pRA58, pRA61, pRA62, pRA63, pRA64, pRA68, pRA74, pRA75, and pRA76 were constructed by site-directed mutagenesis of plasmid pRA50 by using oligo pairs stated in Table S3.

β-galactosidase assays

Overnight grown cultures of the strains were inoculated in LBK broth with pH 6.8 and 8.4 or in LB broth with or without appropriate concentration of $MnCl_2$ at 37°C to a mid-log phase. The appropriate concentration of antibiotics (trimethoprim and/or ampicillin) and IPTG (1 mM) were supplemented when needed in the experiments. β-galactosidase assays were carried out by following the method of Miller, and β-galactosidase-specific activity was reported as Miller units (57). Each reported value of Miller units with a standard error of mean is an average of three biological replicates.

Growth rate measurements

Ten microliters of log-phase cultures of appropriate strain was diluted to 1 mL with fresh LB and LBK media with pH 6.8 and 8.4. The appropriate concentration of $MnCl_2$ was added to LB and LBK media as described in the experiments. Two hundred microliters of these diluted cultures was grown in wells of honeycomb multi-well plates at 37°C while shaking. Growth curves were generated using an automated Spark multimode plate reader by Tecan. In a growth curve, the slope of the graph in the exponential phase was used to calculate the growth rate shown in Table S4.

Cytoplasmic pH measurements

The wild-type strains of *E. coli* and its Δ*alx* mutant containing a plasmid expressing pHluorin (pRA46) were grown overnight in LBK medium buffered with 50 mM of MOPS (pH 7.5) and an appropriate concentration of ampicillin. Cells were inoculated and grown to mid-log phase in fresh LBK medium at pH 7.5 with an appropriate concentration of ampicillin and 1 mM IPTG at 37°C. Cells were harvested from appropriate volume of the cultures by spinning at 4,000 *g*. Cells were resuspended in 4 mL of M63A minimal medium (0.4 g/L KH_2PO_4, 0.4 g/L KH_2PO_4, 2 g/L $(NH_4)_2SO_4$, 7.45 g/L KCl supplemented with 2 g/L casein hydrolysate) and buffered to the desired pH with 50 mM concentration of the appropriate buffer: pH 7.0 and 7.5, MOPS; 8.5, TAPS, and pH 9 and 9.5, AMPSO. Due to poor growth in extremely alkaline conditions, the initial A_{600} for cells growing in M63A media with pH 9 and 9.5 was ~0.2, and in M63A media with external pH (pH_e) 7, 7.5, and 8.5 was ~ 0.05. The cultures were grown for 2 h at 37°C with mild shaking. To generate a standard curve, 95 µL volume of the culture of parent strain expressing pHluorin from each buffered media was withdrawn and mixed with potassium benzoate to a final concentration of 40 mM in 96-well plates. The cultures were incubated at room temperature for 3 min. Methanol amine was added to the culture at a final concentration of 20 mM. The cultures were incubated for 3 min at room temperature. The 100 µL of the parent strain and its Δ*alx* mutant expressing pHluorin were withdrawn from each buffered media to 96 well plates and used for the internal pH (pH_i) measurements. The measurements with fluorescence emission at 530 nm were taken for the two excitation (410 and 470 nm) wavelengths for each strain expressing pHluorin as described in reference (28). The ratio of fluorescence intensity of pHluorin at two excitation wavelengths against pH was plotted to generate a standard curve for the graph. The slope of the curve was used to calculate the pH_i across different pH_e. The data obtained were presented as an average of three biological replicates with standard error of mean.

Tests of the Mn^{2+}-sensitive phenotype and its rescue

Strains were inoculated in LB broth overnight at 37°C in a shaker. Five microliters of tenfold serial dilutions of an overnight grown culture of each strain was spotted on LB agar supplemented with $MnCl_2$ as described in the Results. Whenever required, LB broth or agar media were supplemented with an appropriate concentration of antibiotics and IPTG. LB agar plates were imaged after incubation at 37°C for 14–16 h.

ICP-MS measurement of cellular and media metal ions

The total Mn, Fe, and Zn were quantified from 5 mL cultures. Cells were grown overnight in LB broth and then inoculated in LBK pH 6.8 or LBK pH 8.4 media supplemented with 1 mM IPTG and appropriate concentration of ampicillin. After growth to the mid-log phase at 37°C, cells were harvested using centrifugation at 4,000*g* for 10 min. Cell pellets were washed with 10 mM *N*-2-hydroxyethylpiperazine-*N*-2-ethane sulfonic acid (HEPES) pH 7.5, containing 2 mM EDTA, and then washed twice with 10 mM HEPES as described in reference (14). Cell pellets were dried for 1 h in a centrifuge evaporator. Dried cell pellets were solubilized in 400 µL of 30% (vol/vol) HNO_3 and incubated at 95°C for 10 min. Samples were centrifuged at 20,000*g* for 5 min, prepared for ICP-MS by diluting 300 µL of supernatant of lysed cells into 2.7 mL of 2.5% (vol/vol) HNO_3, and analyzed on an iCAP RQ ICP-MS (Thermo Scientific). Metal ion concentrations are presented as intracellular levels after correction for mean cell volume determined from total protein content (4). The data obtained were presented as an average of three biological replicates with standard error of mean.

For media metal ion measurements, cells containing appropriate plasmids were inoculated in LBK pH 8.4 media supplemented with 1 mM IPTG and appropriate concentration of ampicillin. Cells were harvested after growth to mid-exponential phase (0.4–0.5 OD_{600}) and separated from the media by centrifugation at 4,000*g* for 15 min at room temperature. The media supernatant was filtered using a 0.25-µm filter, and 2.5% (vol/vol) HNO_3 was added to the supernatant. The samples prepared for ICP-MS were diluted before analysis 1:50 to avoid interference from LBK media components with MS. From metal ion measurements in the spent media after exponential cell growth, the [Mn] to [Fe] ratio was calculated. The data plotted for spent media were an average of three biological replicates with standard error of mean. In the case of unused media, three technical replicates were employed to determine an average with standard error of mean.

Preparation and storage of inside-out vesicles

Inside-out vesicles were prepared from the strain RAS42 that lacks *alx* and *mntP*. RAS42 containing an empty vector and its derivatives that express Alx^{HA} or $MntP^{HA}$ from the *trc* promoter were cultivated in 1 L of LB broth with an appropriate concentration of ampicillin at 37°C. The cultures were grown to an OD_{600} of 0.2 and then induced with 1 mM IPTG for P_{trc}-driven expression of Alx^{HA} and $MntP^{HA}$ at 18°C for 12 h. The inside-out vesicles were prepared using procedures identical to those described in reference (58) except aliquots were stored in Buffer B with 10% glycerol, frozen in liquid nitrogen, and stored at –80°C until further use.

Detection of substrate-induced proton release in inside-out membrane vesicles

Kinetic measurements were performed as described in reference (40). Frozen vesicles were thawed on ice. Forty microliters of membrane vesicles was diluted to 2 mL with solution of 50 mM KCl and 10 mM $MgSO_4$. ACMA (10 µM) and valinomycin (0.05 µM) were added at the beginning of the kinetic measurement. The fluorescence measurements of ACMA (λ_{Ex} 409 nm, λ_{Em} 474 nm) were recorded for 250 s with continuous stirring of the samples. ATP (0.25 mM, final concentration) was added after 50 s to generate the

pH gradient across the membrane as estimated by quenching of ACMA's fluorescence. $MnCl_2$ (1 mM, final concentration) was added after 150 s. Any significant change in pH due to substrate-induced proton release was measured by dequenching of ACMA fluorescence. The measurements were terminated by the addition of nigericin (4 µM) after 200 s.

Immunoblotting

The cultures were grown to the mid-log phase. Cells were harvested by centrifugation at 20,000*g* for 1 min. Cell pellets (OD_{600} of 1) were solubilized in 200 µL of SDS-PAGE loading dye. The whole cell extracts were loaded on 12% SDS-PAGE gel after incubation at 37°C for 10 min. Proteins were transferred to the PVDF membrane (Bio-Rad) by Trans-Blot Turbo, a semi-dry transfer apparatus (Bio-Rad). The PVDF membrane was treated with a blocking buffer (Tris-HCl buffer saline with 5% fat-free milk powder) for 30 min. The membrane was probed with an anti-HA rabbit monoclonal antibody (Invitrogen) at a dilution of 1:5,000 overnight at 4°C and with an anti-rabbit, horseradish peroxidase-conjugated antibody (Promega) at a dilution of 1:5,000 for 2 h at room temperature. The blot was developed using a Clarity Western ECL substrate (Bio-Rad), and the signal was detected by the ChemiDoc imaging system. The PVDF membrane was stained with 0.1% amido black solution to confirm equal loading of samples across the lanes. Following staining for 15 s, the membrane was destained with a solution of 45% methanol, 45% water, and 10% glacial acetic acid.

Statistical analysis

Calculations for mean with standard error of mean (SEM) and statistical analyses were performed using GraphPad Prism version 9.5.1 for Windows. The two-way ANOVA test was used for statistical analysis. A *P*-value greater than 0.05 is not considered statistically significant (ns), whereas a *P*-value less that 0.05 is considered significant and indicated by an *. Unless specified in the figures, fold changes are not statistically significant.

ACKNOWLEDGMENTS

We thank Terry Hwa, Abhijit A. Sardesai, James Imlay, and Robert Browne for sharing strains and plasmids for this study. We are grateful to Neal Arakawa at the Environmental and Complex Analysis Laboratory (ECAL) at UCSD for helping with metal ion measurements. We also thank Mark Herzik, Galia Debelouchina, Itay Budin, Elizabeth Komives, and Terry Hwa for providing access to their lab instruments. We thank Iman Saeed for preparing several clones for this study and members of the Mishanina lab for critically reading the manuscript.

This work was supported by the National Institutes of Health (NIGMS ESI grant R35GM142785), UCSD institutional support, and Yinan Wang Memorial Chancellor's Endowed Junior Faculty Fellowship to T.V.M.

AUTHOR AFFILIATION

[1]Department of Chemistry and Biochemistry, University of California San Diego, La Jolla, California, USA

AUTHOR ORCIDs

Ravish Sharma http://orcid.org/0009-0002-0311-6909
Tatiana V. Mishanina http://orcid.org/0000-0001-7400-3501

FUNDING

Funder	Grant(s)	Author(s)
HHS | NIH | National Institute of General Medical Sciences (NIGMS)	R35GM142785	Tatiana V. Mishanina

AUTHOR CONTRIBUTIONS

Ravish Sharma, Conceptualization, Data curation, Formal analysis, Investigation, Methodology, Validation, Visualization, Writing – original draft, Writing – review and editing | Tatiana V. Mishanina, Conceptualization, Funding acquisition, Supervision, Writing – review and editing

ADDITIONAL FILES

The following material is available online.

Supplemental Material

Supplemental material (JB00168-24-s0001.docx). Figures S1 to S8; Tables S1 to S5.

REFERENCES

1. Hopkin KA, Papazian MA, Steinman HM. 1992. Functional differences between manganese and iron superoxide dismutases in *Escherichia coli* K-12. J Biol Chem 267:24253–24258.
2. Anjem A, Varghese S, Imlay JA. 2009. Manganese import is a key element of the OxyR response to hydrogen peroxide in *Escherichia coli*. Mol Microbiol 72:844–858. https://doi.org/10.1111/j.1365-2958.2009.06699.x
3. Patzer SI, Hantke K. 2001. Dual repression by Fe^{2+}-Fur and Mn^{2+}-MntR of the mntH gene, encoding an NRAMP-like Mn^{2+} transporter in *Escherichia coli*. J Bacteriol 183:4806–4813. https://doi.org/10.1128/JB.183.16.4806-4813.2001
4. Martin JE, Waters LS, Storz G, Imlay JA. 2015. The *Escherichia coli* small protein MntS and exporter MntP optimize the intracellular concentration of manganese. PLoS Genet 11:e1004977. https://doi.org/10.1371/journal.pgen.1004977
5. Kaur G, Kumar V, Arora A, Tomar A, Sur R, Dutta D. 2017. Affected energy metabolism under manganese stress governs cellular toxicity. Sci Rep 7:11645. https://doi.org/10.1038/s41598-017-12004-3
6. Kaur G, Sengupta S, Kumar V, Kumari A, Ghosh A, Parrack P, Dutta D. 2014. Novel MntR-independent mechanism of manganese homeostasis in *Escherichia coli* by the ribosome-associated protein HflX. J Bacteriol 196:2587–2597. https://doi.org/10.1128/JB.01717-14
7. Makui H, Roig E, Cole ST, Helmann JD, Gros P, Cellier MFM. 2000. Identification of the *Escherichia coli* K-12 Nramp orthologue (MntH) as a selective divalent metal ion transporter. Mol Microbiol 35:1065–1078. https://doi.org/10.1046/j.1365-2958.2000.01774.x
8. Haemig HAH, Brooker RJ. 2004. Importance of conserved acidic residues in MntH, the Nramp homolog of *Escherichia coli*. J Membr Biol 201:97–107. https://doi.org/10.1007/s00232-004-0711-x
9. Bozzi AT, Zimanyi CM, Nicoludis JM, Lee BK, Zhang CH, Gaudet R. 2019. Structures in multiple conformations reveal distinct transition metal and proton pathways in an Nramp transporter. Elife 8:e41124. https://doi.org/10.7554/eLife.41124
10. Kehres DG, Zaharik ML, Finlay BB, Maguire ME. 2000. The NRAMP proteins of *Salmonella typhimurium* and *Escherichia coli* are selective manganese transporters involved in the response to reactive oxygen. Mol Microbiol 36:1085–1100. https://doi.org/10.1046/j.1365-2958.2000.01922.x
11. Grass G, Franke S, Taudte N, Nies DH, Kucharski LM, Maguire ME, Rensing C. 2005. The metal permease ZupT from *Escherichia coli* is a transporter with a broad substrate spectrum. J Bacteriol 187:1604–1611. https://doi.org/10.1128/JB.187.5.1604-1611.2005
12. Taudte N, Grass G. 2010. Point mutations change specificity and kinetics of metal uptake by ZupT from *Escherichia coli*. Biometals 23:643–656. https://doi.org/10.1007/s10534-010-9319-z
13. Waters LS, Sandoval M, Storz G. 2011. The *Escherichia coli* MntR miniregulon includes genes encoding a small protein and an efflux pump required for manganese homeostasis. J Bacteriol 193:5887–5897. https://doi.org/10.1128/JB.05872-11
14. Zeinert R, Martinez E, Schmitz J, Senn K, Usman B, Anantharaman V, Aravind L, Waters LS. 2018. Structure–function analysis of manganese exporter proteins across bacteria. J Biol Chem 293:5715–5730. https://doi.org/10.1074/jbc.M117.790717
15. Ouyang A, Gasner KM, Neville SL, McDevitt CA, Frawley ER. 2022. MntP and YiiP contribute to manganese efflux in *Salmonella enterica* serovar Typhimurium under conditions of manganese overload and nitrosative stress. Microbiol Spectr 10:e0131621. https://doi.org/10.1128/spectrum.01316-21
16. Serganov A, Nudler E. 2013. A decade of riboswitches. Cell 152:17–24. https://doi.org/10.1016/j.cell.2012.12.024
17. Cromie MJ, Shi Y, Latifi T, Groisman EA. 2006. An RNA sensor for intracellular Mg^{2+}. Cell 125:71–84. https://doi.org/10.1016/j.cell.2006.01.043
18. Dann CE, Wakeman CA, Sieling CL, Baker SC, Irnov I, Winkler WC. 2007. Structure and mechanism of a metal-sensing regulatory RNA. Cell 130:878–892. https://doi.org/10.1016/j.cell.2007.06.051
19. Dambach M, Sandoval M, Updegrove TB, Anantharaman V, Aravind L, Waters LS, Storz G. 2015. The ubiquitous *yybP-ykoY* riboswitch is a manganese-responsive regulatory element. Mol Cell 57:1099–1109. https://doi.org/10.1016/j.molcel.2015.01.035
20. Kalita A, Mishra RK, Kumar V, Arora A, Dutta D. 2022. An intrinsic alkalization circuit turns on *mntP* riboswitch under manganese stress in *Escherichia coli*. Microbiol Spectr 10:e0336822. https://doi.org/10.1128/spectrum.03368-22
21. Meyer MM, Hammond MC, Salinas Y, Roth A, Sudarsan N, Breaker RR. 2011. Challenges of ligand identification for riboswitch candidates. RNA Biol 8:5–10. https://doi.org/10.4161/rna.8.1.13865
22. Breaker RR. 2022. The biochemical landscape of riboswitch ligands. Biochemistry 61:137–149. https://doi.org/10.1021/acs.biochem.1c00765
23. Bingham RJ, Hall KS, Slonczewski JL. 1990. Alkaline induction of a novel gene locus, *alx*, in *Escherichia coli*. J Bacteriol 172:2184–2186. https://doi.org/10.1128/jb.172.4.2184-2186.1990
24. Nechooshtan G, Elgrably-Weiss M, Sheaffer A, Westhof E, Altuvia S. 2009. A pH-responsive riboregulator. Genes Dev 23:2650–2662. https://doi.org/10.1101/gad.552209
25. Anantharaman V, Iyer LM, Aravind L. 2012. Ter-dependent stress response systems: novel pathways related to metal sensing, production of a nucleoside-like metabolite, and DNA-processing. Mol Biosyst 8:3142–3165. https://doi.org/10.1039/c2mb25239b

26. Mishanina TV, Palo MZ, Nayak D, Mooney RA, Landick R. 2017. Trigger loop of RNA polymerase is a positional, not acid-base, catalyst for both transcription and proofreading. Proc Natl Acad Sci U S A 114:E5103–E5112. https://doi.org/10.1073/pnas.1702383114
27. Stephen C, Mishanina TV. 2022. Alkaline pH has an unexpected effect on transcriptional pausing during synthesis of the *Escherichia coli* pH-responsive riboswitch. J Biol Chem 298:102302. https://doi.org/10.1016/j.jbc.2022.102302
28. Martinez KA, Kitko RD, Mershon JP, Adcox HE, Malek KA, Berkmen MB, Slonczewski JL. 2012. Cytoplasmic pH response to acid stress in individual cells of *Escherichia coli* and *Bacillus subtilis* observed by fluorescence ratio imaging microscopy. Appl Environ Microbiol 78:3706–3714. https://doi.org/10.1128/AEM.00354-12
29. Hartmann FSF, Weiß T, Shen J, Smahajcsik D, Savickas S, Seibold GM. 2022. Visualizing the pH in *Escherichia coli* colonies via the sensor protein mCherryEA allows high-throughput screening of mutant libraries. mSystems 7:e0021922. https://doi.org/10.1128/msystems.00219-22
30. Kehres DG, Janakiraman A, Slauch JM, Maguire ME. 2002. Regulation of *Salmonella enterica* serovar Typhimurium *mntH* transcription by H_2O_2, Fe^{2+}, and Mn^{2+}. J Bacteriol 184:3151–3158. https://doi.org/10.1128/JB.184.12.3151-3158.2002
31. Seaver LC, Imlay JA. 2001. Alkyl hydroperoxide reductase is the primary scavenger of endogenous hydrogen peroxide in *Escherichia coli*. J Bacteriol 183:7173–7181. https://doi.org/10.1128/JB.183.24.7173-7181.2001
32. Li X, Imlay JA. 2018. Improved measurements of scant hydrogen peroxide enable experiments that define its threshold of toxicity for *Escherichia coli*. Free Radic Biol Med 120:217–227. https://doi.org/10.1016/j.freeradbiomed.2018.03.025
33. Gottesman S. 1996. Proteases and their targets in *Escherichia coli*. Annu Rev Genet 30:465–506. https://doi.org/10.1146/annurev.genet.30.1.465
34. Laskowska E, Kuczyńska-Wiśnik D, Skórko-Glonek J, Taylor A. 1996. Degradation by proteases Lon, Clp and HtrA, of *Escherichia coli* proteins aggregated *in vivo* by heat shock; HtrA protease action *in vivo* and *in vitro*. Mol Microbiol 22:555–571. https://doi.org/10.1046/j.1365-2958.1996.1231493.x
35. Moon S, Ham S, Jeong J, Ku H, Kim H, Lee C. 2023. Temperature matters: bacterial response to temperature change. J Microbiol 61:343–357. https://doi.org/10.1007/s12275-023-00031-x
36. Pomposiello PJ, Bennik MHJ, Demple B. 2001. Genome-wide transcriptional profiling of the *Escherichia coli* responses to superoxide stress and sodium salicylate. J Bacteriol 183:3890–3902. https://doi.org/10.1128/JB.183.13.3890-3902.2001
37. Veyrier FJ, Boneca IG, Cellier MF, Taha MK. 2011. A novel metal transporter mediating manganese export (MntX) regulates the Mn to Fe intracellular ratio and *Neisseria meningitidis* virulence. PLoS Pathog 7:e1002261. https://doi.org/10.1371/journal.ppat.1002261
38. Daly MJ, Gaidamakova EK, Matrosova VY, Vasilenko A, Zhai M, Venkateswaran A, Hess M, Omelchenko MV, Kostandarithes HM, Makarova KS, Wackett LP, Fredrickson JK, Ghosal D. 2004. Accumulation of Mn(II) in *Deinococcus radiodurans* facilitates gamma-radiation resistance. Science 306:1025–1028. https://doi.org/10.1126/science.1103185
39. Helmann JD. 2014. Specificity of metal sensing: iron and manganese homeostasis in *Bacillus subtilis*. J Biol Chem 289:28112–28120. https://doi.org/10.1074/jbc.R114.587071
40. Dubey S, Majumder P, Penmatsa A, Sardesai AA. 2021. Topological analyses of the L-lysine exporter LysO reveal a critical role for a conserved pair of intramembrane solvent-exposed acidic residues. J Biol Chem 297:101168. https://doi.org/10.1016/j.jbc.2021.101168
41. Stancik LM, Stancik DM, Schmidt B, Barnhart DM, Yoncheva YN, Slonczewski JL. 2002. pH-dependent expression of periplasmic proteins and amino acid catabolism in *Escherichia coli*. J Bacteriol 184:4246–4258. https://doi.org/10.1128/JB.184.15.4246-4258.2002
42. Whittaker MM, Mizuno K, Bächinger HP, Whittaker JW. 2006. Kinetic analysis of the metal binding mechanism of *Escherichia coli* manganese superoxide dismutase. Biophys J 90:598–607. https://doi.org/10.1529/biophysj.105.071308
43. Li Y, Moe PC, Chandrasekaran S, Booth IR, Blount P. 2002. Ionic regulation of MscK, a mechanosensitive channel from *Escherichia coli*. EMBO J 21:5323–5330. https://doi.org/10.1093/emboj/cdf537
44. Sharma R, Shimada T, Mishra VK, Upreti S, Sardesai AA. 2016. Growth inhibition by external potassium of *Escherichia coli* lacking PtsN (EIIANtr) is caused by potassium limitation mediated by YcgO. J Bacteriol 198:1868–1882. https://doi.org/10.1128/JB.01029-15
45. Roe AJ, McLaggan D, O'Byrne CP, Booth IR. 2000. Rapid inactivation of the *Escherichia coli* Kdp K^+ uptake system by high potassium concentrations. Mol Microbiol 35:1235–1243. https://doi.org/10.1046/j.1365-2958.2000.01793.x
46. Bosma EF, Rau MH, van Gijtenbeek LA, Siedler S. 2021. Regulation and distinct physiological roles of manganese in bacteria. FEMS Microbiol Rev 45:fuab028. https://doi.org/10.1093/femsre/fuab028
47. Paruthiyil S, Pinochet-Barros A, Huang X, Helmann JD. 2020. *Bacillus subtilis* TerC family proteins help prevent manganese intoxication. J Bacteriol 202:e00624-19. https://doi.org/10.1128/JB.00624-19
48. Guedon E, Helmann JD. 2003. Origins of metal ion selectivity in the DtxR/MntR family of metalloregulators. Mol Microbiol 48:495–506. https://doi.org/10.1046/j.1365-2958.2003.03445.x
49. McGuire AM, Cuthbert BJ, Ma Z, Grauer-Gray KD, Brunjes Brophy M, Spear KA, Soonsanga S, Kliegman JI, Griner SL, Helmann JD, Glasfeld A. 2013. Roles of the A and C sites in the manganese-specific activation of MntR. Biochemistry 52:701–713. https://doi.org/10.1021/bi301550t
50. He B, Sachla AJ, Helmann JD. 2023. TerC proteins function during protein secretion to metalate exoenzymes. Nat Commun 14:6186. https://doi.org/10.1038/s41467-023-41896-1
51. Hayes ET, Wilks JC, Sanfilippo P, Yohannes E, Tate DP, Jones BD, Radmacher MD, BonDurant SS, Slonczewski JL. 2006. Oxygen limitation modulates pH regulation of catabolism and hydrogenases, multidrug transporters, and envelope composition in *Escherichia coli* K-12. BMC Microbiol 6:89. https://doi.org/10.1186/1471-2180-6-89
52. Litvak Y, Byndloss MX, Bäumler AJ. 2018. Colonocyte metabolism shapes the gut microbiota. Science 362:eaat9076. https://doi.org/10.1126/science.aat9076
53. Rogers AWL, Tsolis RM, Bäumler AJ. 2020. *Salmonella* versus the microbiome. Microbiol Mol Biol Rev 85:e00027-19. https://doi.org/10.1128/MMBR.00027-19
54. Datsenko KA, Wanner BL. 2000. One-step inactivation of chromosomal genes in *Escherichia coli* K-12 using PCR products. Proc Natl Acad Sci U S A 97:6640–6645. https://doi.org/10.1073/pnas.120163297
55. Baba T, Ara T, Hasegawa M, Takai Y, Okumura Y, Baba M, Datsenko KA, Tomita M, Wanner BL, Mori H. 2006. Construction of *Escherichia coli* K-12 in-frame, single-gene knockout mutants: the Keio collection. Mol Syst Biol 2:2006.0008. https://doi.org/10.1038/msb4100050
56. Larson MH, Mooney RA, Peters JM, Windgassen T, Nayak D, Gross CA, Block SM, Greenleaf WJ, Landick R, Weissman JS. 2014. A pause sequence enriched at translation start sites drives transcription dynamics *in vivo*. Science 344:1042–1047. https://doi.org/10.1126/science.1251871
57. Miller JH. 1992. A short course in bacterial genetics: a laboratory manual and handbook for *Escherichia coli* and related bacteria. Cold Spring Harbor Laboratory, Cold Spring Harbor, NY.
58. Verkhovskaya M. 2017. Preparation of everted membrane vesicles from *Escherichia coli* cells. Bio Protoc 7:e2254. https://doi.org/10.21769/BioProtoc.2254